First, increasing the availability of MSC-derived EVs is of critical importance. Elucidation of the basic mechanisms of EV biogenesis and secretion is key to this issue. It is known that a p53-regulated gene product, TSAP6, enhances EV production in cells undergoing a p53 response to stress [146,147]. Several other intracellular proteins, such as diacylglycerol kinase-α [148] and brefeldin A-inhibited guanine-nucleotide exchange protein 2 [149], have also been proposed to have a role in the secretion of EVs. In addition, the pH of the microenvironment has been reported to regulate EV release in cancer cells [150]. Recent studies have found several molecules that play more general roles in EV biogenesis and secretion [19,20]. Modulating the expression of these genes or the pH of the microenvironment may result in increased EV production by MSCs. Care should be taken, however, because such treatment of MSCs may induce phenotypic changes in parent MSCs that may impair the therapeutic efficacy of any produced EVs. Thus, to boost the availability of MSC-derived EVs, it is important to increase MSC EV production while maintaining normal MSC phenotypes.

Second, specific delivery of MSC-derived EVs to target cells or organs is crucial. One possible approach to this issue is to modify the EV surface to target specific receptors on recipient cells. By fusing the EV membrane protein Lamp2b to peptides that bind to receptors expressed on specific cell types, Alvarez-Erviti et al. observed specific delivery of siRNAs to muscular and neural cells, respectively [151]. In addition, a better understanding of the mechanism for EV uptake may help us improve the efficiency of EV delivery. Considering the tropism of EVs for target cells, it seems possible to improve the efficiency of EV delivery as well as to circumvent nonspecific delivery to unwanted cells or organs. At this moment, however, EV uptake mechanisms other than those of the immune system remain unclear. Several studies have demonstrated that EVs can be taken up by immune cells through phagocytosis [152–154]. In contrast, the mechanisms underlying EV uptake in nonimmune cells are unclear. To improve EV delivery to specific tissues, future work could focus on elucidating EV uptake mechanisms.

Third, enhancing the therapeutic efficiency of MSC-derived EVs will increase the feasibility of their clinical application. One possible approach to this is to increase the amount of specific molecules such as mRNAs, miRNAs, and proteins in EVs through overexpressing them in parent MSCs using genetic modification. This idea is based on the fact that EV contents, at least in part, repeat those of parent cells. Indeed, our group showed that overexpression of a specific miRNA in parent cells leads to an increased secretion of the miRNA into the EVs [16]. Ciravolo et al. also observed that overexpression of human epidermal growth factor receptor2 protein in breast cancer cell lines leads to high expression of human epidermal growth factor receptor 2 in the released EVs [155]. Thus, in the case where the specific molecules necessary for a therapeutic effect are known, selective overexpression of those molecules in the parent MSCs may lead to an enhancement of the therapeutic efficiency of the EVs.

Another and more interesting possibility is global enhancement of the therapeutic potential of MSC-derived EVs. As described above, MSCs can respond to pathological stimuli and secrete various trophic factors required for tissue repair. Considering that EVs can contain many molecules that play certain biological roles, it is possible that in response to a pathological stimulus, MSCs can release EVs loaded with a set of molecules required for tissue repair. This suggests that exposure of MSCs to injury stimuli such as inflammatory cytokines may allow enrichment of a global set of trophic molecules in the released EVs. Furthermore, appropriate preconditioning of parent MSCs with injury stimuli related to a specific disease may allow the tailoring of EV contents to efficiently support repair of specific diseases. To this end, a recapitulation of injury stimuli based on a comprehensive understanding of the injury mechanism will be key to enhancement of the therapeutic efficiency of MSC EVs. On another front, it will be also important to extend the half-lives of EVs. Although information is currently lacking on local concentrations and half lives of EVs in tissues, it is possible that EVs are rapidly cleared by the mononuclear phagocytic system especially when the EVs involve exogenous modification. Recent advances in liposome technology will provide useful insights into this issue [156].

In summary, we propose a general strategy for clinical application of MSC-derived EVs (Fig. 3). The first step is to prepare MSCs by obtaining them from the patient himself/herself or from an allogeneic donor. The use of MSCs for clinical purposes takes advantage of their poor immunogenicity, which supports the possible use of MSCs obtained from allogeneic donors in the clinic [110]. The second step is to expand the prepared MSCs to obtain the required amount of EVs. During this step, optional treatments or gene engineering of the cultured MSCs may allow modification of EVs for selective delivery and/or enhancement of the therapeutic potential of the produced EVs. The third step is to harvest the EVs from the MSC-CM. Upon EV harvest, it will be possible to modify the harvested EVs by packaging siRNA, miRNA, and mRNA into the EVs [151], or loading the EVs with therapeutic drugs [157]. The final step is to administer MSC-derived EVs with therapeutic efficacy to the patient. For efficient delivery of the MSC-derived EVs, researchers are required to explore the best route of administration according to the target disease. Of note, recent reports suggest that EVs administered intravenously [151] or intranasally [157] cross the blood–brain barrier and result in successful delivery of the cargo directly into the brain.

Finally, we caution that researchers in this field should be mindful of safety issues regarding the clinical application of MSC-derived EVs. Despite increasing evidence for the therapeutic efficacy of MSC-derived EVs, this research field is still immature and much remains unclear. In particular, most of the molecules responsible for the therapeutic effects of MSC-derived EVs have yet to be characterized (Table 1). Toward realization of a clinical application for MSC-derived EVs, identification of the necessary molecules is required to

elucidate the mechanisms underlying MSC-EV-mediated therapeutics. Furthermore, it is especially important to carefully investigate whether MSC-derived EVs cause any side effects in animal experiments and preclinical tests. Therefore, future research must not only explore the novel therapeutic potential of MSC-derived EVs, but also carefully evaluate its safety and efficacy.

We thank Dr. Tomohiro Fujiwara for helping us prepare figures. This study was supported in part by a Grant-in-Aid for the Third-Term Comprehensive 10-Year Strategy for Cancer Control of Japan, a grant-in-aid for Scientific Research on Priority Areas Cancer from the Japanese Ministry of Education, Culture, Sports, Science, and Technology, a Grant-in-Aid for cancer research promotion from National Cancer Center of Japan, Grant-in-Aid for Japan Society for the Promotion of Science (JSPS) Fellows, the Program for Promotion of Fundamental Studies in Health Sciences of the National Institute of Biomedical Innovation (NiBio) of Japan, Japan Science and Technology Agency (JST) CREST, and Grant-in-Aid for Scientific Research on Innovative Areas ("functional machinery for non-coding RNAs") from the Japanese Ministry of Education, Culture, Sports, Science, and Technology.

The authors have declared no conflict of interest.

7 References

[1] Behnke, O., An electron microscope study of the megacaryocyte of the rat bone marrow. I. The development of the demarcation membrane system and the platelet surface coat. *J. Ultrastruct. Res.* 1968, *24*, 412–433.

[2] Théry, C., Exosomes: secreted vesicles and intercellular communications. *F1000 Biol. Rep.* 2011, *3*, 15.

[3] Cocucci, E., Racchetti, G., Meldolesi, J., Shedding microvesicles: artefacts no more. *Trends Cell Biol.* 2009, *19*, 43–51.

[4] Harding, C., Heuser, J., Stahl, P., Receptor-mediated endocytosis of transferrin and recycling of the transferrin receptor in rat reticulocytes. *J. Cell Biol.* 1983, *97*, 329–339.

[5] Johnstone, R. M., Adam, M., Hammonds, J. R., Turbide, C., Vesicle formation during reticulocyte maturation. *J. Biol. Chem.* 1987, *262*, 9412–9420.

[6] Johnstone, R. M., Bianchini, A., Teng, K., Reticulocyte maturation and exosome release: transferrin receptor containing exosomes shows multiple plasma membrane functions. *Blood* 1989, *74*, 1844–1851.

[7] Johnstone, R. M., Mathew, A., Mason, A. B., Teng, K., Exosome formation during maturation of mammalian and avian reticulocytes: evidence that exosome release is amajorroute for externalization of obsolete membrane proteins. *J. Cell. Physiol.* 1991, *147*, 27–36.

[8] Johnstone, R. M., The Jeanne Manery-Fisher Memorial Lecture 1991. Maturation of reticulocytes: formation of exosomes as a mechanism for shedding membrane proteins. *Biochem. Cell Biol.* 1992, *70*, 179–190.

[9] Taylor, D. D., Homesley, H. D., Doellgast, G. J., Binding of specific peroxidase-labeled antibody to placental-type phosphatase on tumor-derived membrane fragments. *Cancer Res.* 1980 *40*, 4064–4069.

[10] Camussi, G., Deregibus, M. C., Bruno, S., Cantaluppi, V., Biancone, L., Exosomes/microvesicles as a mechanism of cell-to-cell communication. *Kidney Int.* 2010, *78*, 838–848.

[11] Raposo, G., Nijman, H. W., Stoorvogel, W., Liejendekker, R. et al., B lymphocytes secrete antigen-presenting vesicles. *J. Exp. Med.* 1996, *183*, 1161–1172.

[12] Ratajczak, J., Miekus, K., Kucia, M., Zhang, J. et al., Embryonic stem cell-derived microvesicles reprogram hematopoietic progenitors: evidence for horizontal transfer of mRNA and protein delivery. *Leukemia* 2006, *20*, 847–856.

[13] Valadi, H., Ekström, K., Bossios, A., Sjöstrand, M. et al., Exosome-mediated transfer of mRNAs and microRNAs is a novel mechanism of genetic exchange between cells. *Nat. Cell Biol.* 2007, *9*, 654–659.

[14] Pegtel, D. M., Cosmopoulos, K., Thorley-Lawson, D. A, van Eijndhoven, M. A. et al., Functional delivery of viral miRNAs via exosomes. *Proc. Natl. Acad. Sci. USA* 2010, *107*, 6328–6333.

[15] Zhang, Y., Liu, D., Chen, X., Li, J. et al., Secreted monocytic miR-150 enhances targeted endothelial cell migration. *Mol. Cell.* 2010, *39*, 133–144.

[16] Kosaka, N., Iguchi, H., Yoshioka, Y., Takeshita, F. et al., Secretory mechanisms and intercellular transfer of microRNAs in living cells. *J. Biol. Chem.* 2010, *285*, 17442–17452.

[17] Théry, C., Zitvogel, L., Amigorena, S., Exosomes: composition, biogenesis and function. *Nat. Rev. Immunol.* 2002, *2*, 569–579.

[18] Savina, A., Furlán, M., Vidal, M., Colombo, M. I., Exosome release is regulated by a calcium-dependent mechanism in K562 cells. *J. Biol. Chem.* 2003, *278*, 20083–20090.

[19] Trajkovic, K., Hsu, C., Chiantia, S., Rajendran, L. et al., Ceramide triggers budding of exosome vesicles into multivesicular endosomes. *Science* 2008, *319*, 1244–1247.

[20] Ostrowski, M., Carmo, N. B., Krumeich, S., Fanget, I. et al., Rab27a and Rab27b control different steps of the exosome secretion pathway. *Nat. Cell Biol.* 2010, *12*, 19–30.

[21] Taylor, D. D., Gercel-Taylor, C., MicroRNA signatures of tumor-derived exosomes as diagnostic biomarkers of ovarian cancer. *Gynecol. Oncol.* 2008, *110*, 13–21.

[22] Sheldon, H., Heikamp, E., Turley, H., Dragovic, R. et al., New mechanism for Notch signaling to endothelium at a distance by Delta-like 4 incorporation into exosomes. *Blood* 2010, *116*: 2385–2394.

[23] Zitvogel, L., Regnault, A., Lozier, A., Wolfers, J. et al., Eradication of established murine tumors using a novel cell-free vaccine: dendritic cell derived exosomes. *Nat. Med.* 1998, *4*, 594–600.

[24] Skokos, D., Le Panse, S., Villa, I., Rousselle, J. C. et al., Mast cell-dependent B and T lymphocyte activation is mediated by the secretion of immunologically active exosomes. *J. Immunol.* 2001, *166*, 868–876.

[25] Skokos, D., Botros, H. G., Demeure, C., Morin, J. et al., Mast cell-derived exosomes induce phenotypic and functional maturation of dendritic cells and elicit specific immune responses in vivo. *J. Immunol.* 2003, *170*, 3037–3045.

[26] Mittelbrunn, M., Gutiérrez-Vázquez, C., Villarroya-Beltri, C., González, S. et al., Unidirectional transfer of microRNA-loaded exosomes from T cells to antigen-presenting cells. *Nat. Commun.* 2011, *2*, 282.

[27] Dunn, G. P., Bruce, A. T., Ikeda, H., Old, L. J., Schreiber, R. D., Cancer immunoediting : from immuno-surveillance to tumor escape. *Nat. Immunol.* 2002, *3*, 991–998.

[28] Dunn, G. P., Old, L. J., Schreiber, R. D., The three Es of cancer immunoediting. *Annu. Rev. Immunol.* 2004, *22*, 329–360.

[29] Wolfers, J., Lozier, A., Raposo, G., Regnault, A. et al., Tumor-derived exosomes are a source of shared tumor rejection antigens for CTL cross-priming. *Nat. Med.* 2001, *7*, 297–303.

[30] Zeelenberg, I. S., Ostrowski, M., Krumeich, S., Bobrie, A. et al., Targeting tumor antigens to secreted membrane vesicles in vivo induces efficient antitumor immune responses. *Cancer Res.* 2008, *68*, 1228–1235.

[31] Gastpar, R., Gehrmann, M., Bausero, M. A., Asea, A. et al., Heat shock protein 70 surface-positive tumor exosomes stimulate migratory and cytolytic activity of natural killer cells. *Cancer Res.* 2005, *65*, 5238–5247.

[32] Andreola, G., Rivoltini, L., Castelli, C., Huber, V. et al., Induction of lymphocyte apoptosis by tumor cell secretion of FasL-bearing microvesicles. *J. Exp. Med.* 2002, *195*, 1303–1316.

[33] Abusamra, A. J., Zhong, Z., Zheng, X., Li, M. et al., Tumor exosomes expressing Fas ligand mediate CD8+ T-cell apoptosis. *Blood Cells Mol. Dis.* 2005, *35*, 169–173.

[34] Clayton, A., Mitchell, J. P., Court, J., Mason, M. D., Tabi, Z., Human tumor-derived exosomes selectively impair lymphocyte responses to interleukin-2. Responses to interleukin-2. *Cancer Res.* 2007, *67*, 7458–7466.

[35] Chalmin, F., Ladoire, S., Mignot, G., Vincent, J. et al., Membrane-associated Hsp72 from tumor-derived exosomes mediates STAT3-dependent immunosuppressive function of mouse and human myeloid-derived suppressor cells. *J. Clin. Invest.* 2010, *120*, 457–471.

[36] Gutwein, P., Stoeck, A., Riedle, S., Gast, D. et al., Cleavage of L1 in exosomes and apoptotic membrane vesicles released from ovarian carcinoma cells. *Clin. Cancer Res.* 2005, *11*, 2492–2501.

[37] Higginbotham, J. N., Demory Beckler, M., Gephart, J. D., Franklin, J. L. et al., Amphiregulin exosomes increase cancer cell invasion. *Curr. Biol.* 2011, *21*, 779–786.

[38] Biernat, W., Huang, H., Yokoo, H., Kleihues, P., Ohgaki, H., Predominant expression of mutant EGFR (EGFRvIII) is rare in primary glioblastomas. *Brain Pathol.* 2004, *14*, 131–136.

[39] Al-Nedawi, K., Meehan, B., Micallef, J., Lhotak, V. et al., Intercellular transfer of the oncogenic receptor EGFRvIII by microvesicles derived from tumour cells. *Nat. Cell Biol.* 2008, *10*, 619–624.

[40] Skog, J., Würdinger, T., van Rijn, S., Meijer, D. H. et al., Glioblastoma microvesicles transport RNA and proteins that promote tumour growth and provide diagnostic biomarkers. *Nat. Cell Biol.* 2008, *10*, 1470–1476.

[41] Gesierich, S., Berezovskiy, I., Ryschich, E., Zöller, M., Systemic induction of the angiogenesis switch by the tetraspanin D6.1A/CO-029. *Cancer Res.* 2006, *66*, 7083–7094.

[42] Nazarenko, I., Rana, S., Baumann, A., Mcalear, J. et al., Cell surface tetraspanin Tspan8 contributes to molecular pathways of exosome-induced endothelial cell activation. *Cancer Res.* 2010, *70*, 1668–1678.

[43] Al-Nedawi, K., Meehan, B., Kerbel, R. S., Allison, A. C., Rak, J., Endothelial expression of autocrine VEGF upon the uptake of tumor-derived microvesicles containing oncogenic EGFR. *Proc. Natl. Acad. Sci. USA* 2009, *106*, 3794–3799.

[44] Kaplan, R. N., Riba, R. D., Zacharoulis, S., Bramley, A. H. et al., VEGFR1-positive haematopoietic bone marrow progenitors initiate the pre-metastatic niche. *Nature* 2005, *438*, 820–827.

[45] Peinado, H., Alečković, M., Lavotshkin, S., Matei, I. et al., Melanoma exosomes educate bone marrow progenitor cells toward a pro-metastatic phenotype through MET. *Nat. Med.* 2012, *18*, 883–891.

[46] Jung, T., Castellana, D., Klingbeil, P., Cuesta Hernández, I. et al., CD44v6 dependence of premetastatic niche preparation by exosomes. *Neoplasia* 2009, *11*, 1093–1105.

[47] Deregibus, M. C., Cantaluppi, V., Calogero, R., Lo Iacono, M. et al., Endothelial progenitor cell derived microvesicles activate an angiogenic program in endothelial cells by a horizontal transfer of mRNA. *Blood* 2007, *110*, 2440–2448.

[48] Kosaka, N., Iguchi, H., Yoshioka, Y., Hagiwara, K. et al., Competitive interactions of cancer cells and normal cells via secretory microRNAs. *J. Biol. Chem.* 2011, *287*, 1397–1405.

[49] Katsuda, T., Sakai, Y., Ochiya, T., Induced pluripotent stem cell-derived hepatocytes as an alternative to human adult hepatocytes. *J. Stem Cells.* 2012, *7*, 1–17.

[50] Yamanaka, S., A fresh look at iPS cells. *Cell* 2009, *137*, 13–17.

[51] Fairchild, P. J., The challenge of immunogenicity in the quest for induced pluripotency. *Nat. Rev. Immunol.* 2010, *10*, 868–875.

[52] Chamberlain, G., Fox, J., Ashton, B., Middleton, J., Concise review: mesenchymal stem cells: their phenotype, differentiation capacity, immunological features, and potential for homing. *Stem Cells* 2007, *25*, 2739–2749.

[53] Djouad, F., Bouffi, C., Ghannam, S., Noël, D., Jorgensen, C., Mesenchymal stem cells: innovative therapeutic tools for rheumatic diseases. *Nat. Rev. Rheumatol.* 2009, *5*, 392–399.

[54] Salem, H. K., Thiemermann, C., Mesenchymal stromal cells: current understanding and clinical status. *Stem Cells* 2010, *28*, 585–596.

[55] Psaltis, P. J., Zannettino, A. C. W., Worthley, S. G., Gronthos, S., Concise review: mesenchymal stromal cells: potential for cardiovascular repair. *Stem Cells* 2008, *26*, 2201–2210.

[56] Ochiya, T., Yamamoto, Y., Banas, A., Commitment of stem cells into functional hepatocytes. *Differentiation* 2010, *79*, 65–73.

[57] Friedenstein, A. J., Chailakhyan, R. K., Latsinik, N. V., Panasyuk, A. F., Keiliss-Borok, I. V., Stromal cells responsible for transferring the microenvironment of the hemopoietic tissues. Cloning in vitro and retransplantation in vivo. *Transplantation* 1974, *17*, 331–340.

[58] Friedenstein, A. J., Gorskaja, J. F., Kulagina, N. N., Fibroblast precursors in normal and irradiated mouse hematopoietic organs. *Exp. Hematol.* 1976, *4*, 267–274.

[59] Dominici, M., Le Blanc, K., Mueller, I., Slaper-Cortenbach, I. et al., Minimal criteria for defining multipotent mesenchymal stromal cells. The International Society for Cellular Therapy position statement. *Cytotherapy* 2006, *8*, 315–317.

[60] Phinney, D. G., Prockop, D. J., Concise review: mesenchymal stem/multipotent stromal cells: the state of transdifferentiation and modes of tissue repair–current views. *Stem Cells* 2007, *25*, 2896–2902.

[61] Zhang, Y., Wang, W., Effects of bone marrow mesenchymal stem cell transplantation on light-damaged retina. *Invest. Ophthalmol. Vis. Sci.* 2010, *51*, 3742–3748.

[62] Shi, C., Zhu, Y., Su, Y., Cheng, T., Stem cells and their applications in skin-cell therapy. *Trends Biotechnol.* 2006, *24*, 48–52.

[63] Banas, A., Yamamoto, Y., Teratani, T., Ochiya, T., Stem cell plasticity: learning from hepatogenic differentiation strategies. *Dev. Dyn.* 2007, *236*, 3228–3241.

[64] Humphreys, B. D., Bonventre, J. V., Mesenchymal stem cells in acute kidney injury. *Annu. Rev. Med.* 2008, *59*, 311–325.

[65] Kotton, D. N., Ma, B. Y., Cardoso, W. V., Sanderson, E. A. et al., Bone marrow-derived cells as progenitors of lung alveolar epithelium. *Development* 2001, *128*, 5181–5188.

[66] Ortiz, L.A., Gambelli, F., McBride, C., Gaupp, D. et al., Mesenchymal stem cell engraftment in lung is enhanced in response to bleomycin exposure and ameliorates its fibrotic effects. *Proc. Natl. Acad. Sci. USA* 2003, *100*, 8407–8411.

[67] Gage, F. H., Mammalian neural stem cells. *Science* 2000, *287*, 1433–1438.

[68] Kopen, G. C., Prockop, D. J., Phinney, D.G., Marrow stromal cells migrate throughout forebrain and cerebellum, and they differentiate into astrocytes after injection into neonatal mouse brains. *Proc. Natl. Acad. Sci. USA* 1999, *96*, 10711–10716.

[69] Chen, J., Li, Y., Wang, L., Lu, M. et al., Therapeutic benefit of intracerebral transplantation of bone marrow stromal cells after cerebral ischemia in rats. *J. Neurol. Sci.* 2001, *189*, 49–57.

[70] Zhao, L. R., Duan, W. M., Reyes, M., Keene, C. D. et al., Human bone marrow stem cells exhibit neural phenotypes and ameliorate neurological deficits after grafting into the ischemic brain of rats. *Exp. Neurol.* 2002, *174*, 11–20.

[71] Muñoz-Elias, G., Marcus, A. J., Coyne, T. M., Woodbury, D., Black, I. B., Adult bone marrow stromal cells in the embryonic brain: engraftment, migration, differentiation, and long-term survival. *J. Neurosci.* 2004, *24*, 4585–4895.

[72] Sanchez-Ramos, J., Song, S., Cardozo-Pelaez, F., Hazzi, C. et al., Adult bone marrow stromal cells differentiate into neural cells in vitro. *Exp. Neurol.* 2000, *164*, 247–256.

[73] Woodbury, D., Schwarz, E. J., Prockop, D. J., Black, I. B., Adult rat and human bone marrow stromal cells differentiate into neurons. *J. Neurosci. Res.* 2000, *61*, 364–370.

[74] Kitada M, Dezawa, M., Induction system of neural and muscle lineage cells from bone marrow stromal cells; a new strategy for tissue reconstruction in degenerative diseases. *Histol. Histopathol. [Internet]* 2009, *24*(5), 631–642.

[75] Fisher, R. A., Strom, S. C., Human hepatocyte transplantation: worldwide results. *Transplantation* 2006, *82*, 441–449.

[76] Carpentier, B., Gautier, A., Legallais, C., Artificial and bioartificial liver devices: present and future. *Gut.* 2009, *58*, 1690–1702.

[77] Sakai, Y., Nishikawa, M., Evenou, F., Hamon, M. et al., Engineering of implantable liver tissues. *Methods Mol. Biol.* 2012, *826*, 189–216.

[78] Teratani, T., Yamamoto, H., Aoyagi, K., Sasaki, H. et al., Direct hepatic fate specification from mouse embryonic stem cells. *Hepatology* 2005, *41*, 836–846.

[79] Soto-Gutiérrez, A., Kobayashi, N., Rivas-Carrillo, J. D., Navarro-Alvarez, N. et al., Reversal of mouse hepatic failure using an implanted liver-assist device containing ES cell-derived hepatocytes. *Nat. Biotechnol.* 2006, *24*, 1412–1419.

[80] Cai, J., Zhao, Y., Liu, Y., Ye, F. et al., Directed differentiation of human embryonic stem cells into functional hepatic cells. *Hepatology* 2007, *45*, 1229–1239.

[81] Si-Tayeb, K., Noto, F. K., Nagaoka, M., Li, J. et al., Highly efficient generation of human hepatocyte-like cells from induced pluripotent stem cells. *Hepatology* 2010, *51*, 297–305.

[82] Sullivan, G. J., Hay, D. C., Park, I. H., Fletcher, J. et al., Generation of functional human hepatic endoderm from human induced pluripotent stem cells. *Hepatology* 2010, *51*, 329–335.

[83] Touboul, T., Hannan, N. R. F., Corbineau, S., Martinez, A. et al., Generation of functional hepatocytes from human embryonic stem cells under chemically defined conditions that recapitulate liver development. *Hepatology* 2010, *51*, 1754–1765.

[84] Kamiya, A., Kojima, N., Kinoshita, T., Sakai, Y., Miyaijma, A., Maturation of fetal hepatocytes in vitro by extracellular matrices and oncostatin M: induction of tryptophan oxygenase. *Hepatology* 2002, *35*, 1351–1359.

[85] Hanada, S., Kojima, N., Sakai, Y., Soluble factor-dependent in vitro growth and maturation of rat fetal liver cells in a three-dimensional culture system. *Tissue Eng. Part A* 2008, *14*, 149–160.

[86] Katsuda, T., Teratani, T., Ochiya, T., Sakai, Y., Transplantation of a fetal liver cell-loaded hyaluronic acid sponge onto the mesentery recovers a Wilson's disease model rat. *J. Biochem.* 2010, *148*, 281–288.

[87] Lázaro, C. A., Rhim, J. A., Yamada, Y., Lã, C. A. et al., Generation of hepatocytes from oval cell precursors in culture. *Cancer Res.* 1998, *58*, 5514–5522.

[88] Yovchev, M. I., Grozdanov, P. N., Zhou, H., Racherla, H. et al., Identification of adult hepatic progenitor cells capable of repopulating injured rat liver. *Hepatology* 2008, *47*, 636–647.

[89] Sudo, R., Mitaka, T., Ikeda, M., Tanishita, K., Reconstruction of 3D stacked-up structures by rat small hepatocytes on microporous membranes. *FASEB J.* 2005, *19*, 1695–1697.

[90] Dollé, L., Best, J., Mei, J., Al Battah, F., Reynaert, H. et al., The quest for liver progenitor cells: a practical point of view. *J. Hepatol.* 2010, *52*, 117–129.

[91] Lee, K. D., Kuo, T. K., Whang-Peng, J., Chung, Y. F. et al., In vitro hepatic differentiation of human mesenchymal stem cells. *Hepatology* 2004, *40*, 1275–1284.

[92] Lee, O. K., Kuo, T. K., Chen, W. M., Lee, K. D. et al., Isolation of multipotent mesenchymal stem cells from umbilical cord blood. *Blood* 2004, *103*, 1669–1675.

[93] Sato, Y., Araki, H., Kato, J., Nakamura, K. et al., Human mesenchymal stem cells xenografted directly to rat liver are differentiated into human hepatocytes without fusion. *Blood* 2005, *106*, 756–763.

[94] Hong, S. H., Gang, E. J., Jeong, J. A., Ahn, C. et al., In vitro differentiation of human umbilical cord blood-derived mesenchymal stem cells into hepatocyte-like cells. *Biochem. Biophys. Res. Commun.* 2005, *330*, 1153–1161

[95] Aurich, I., Mueller, L. P., Aurich, H., Luetzkendorf, J. et al., Functional integration of hepatocytes derived from human mesenchymal stem cells into mouse livers. *Gut* 2007, *56*, 405–415.

[96] Seo, M. J., Suh, S. Y., Bae, Y. C., Jung, J. S., Differentiation of human adipose stromal cells into hepatic lineage in vitro and in vivo. *Biochem. Biophys. Res. Commun.* 2005, *328*, 258–264.

[97] Taléns-Visconti, R., Bonora, A., Jover, R., Mirabet, V. et al., Hepatogenic differentiation of human mesenchymal stem cells from adipose tissue in comparison with bone marrow mesenchymal stem cells. *World J. Gastroenterol.* 2006, *12*, 5834–5845.

[98] Banas, A., Teratani, T., Yamamoto, Y., Tokuhara, M. et al., Adipose tissue-derived mesenchymal stem cells as a source of human hepatocytes. *Hepatology* 2007, *46*, 219–228.

[99] Banas, A., Teratani, T., Yamamoto, Y., Tokuhara, M. et al., Rapid hepatic fate specification of adipose-derived stem cells and their therapeutic potential for liver failure. *J. Gastroenterol. Hepatol.* 2009, *24*, 70–77

[100] Yamamoto, Y., Banas, A., Murata, S., Ishikawa, M. et al., A comparative analysis of the transcriptome and signal pathways in hepatic differentiation of human adipose mesenchymal stem cells. *FEBS J.* 2008, *275*, 1260–1273.

[101] Banas, A., Teratani, T., Yamamoto, Y., Tokuhara, M. et al., IFATS collection: in vivo therapeutic potential of human adipose tissue mesenchymal stem cells after transplantation into mice with liver injury. *Stem Cells* 2008, *26*, 2705–2712.

[102] Parekkadan, B., van Poll, D., Suganuma, K., Carter, E. A. et al., Mesenchymal stem cell-derived molecules reverse fulminant hepatic failure. *PLoS One* 2007, *2*, e941.

[103] van Poll, D., Parekkadan, B., Cho, C. H., Berthiaume, F. et al., Mesenchymal stem cell-derived molecules directly modulate hepatocellular death and regeneration in vitro and in vivo. *Hepatology* 2008, *47*, 1634–40163.

[104] Kuo, T. K., Hung, S. P., Chuang, C. H, Chen, C. T. et al., Stem cell therapy for liver disease: parameters governing the success of using bone marrow mesenchymal stem cells. *Gastroenterology* 2008, *134*, 2111–2121.

[105] Zappia, E., Casazza, S., Pedemonte, E., Benvenuto, F. et al., Mesenchymal stem cells ameliorate experimental autoimmune encephalomyelitis inducing T-cell anergy. *Blood* 2005, *106*, 1755–1761.

[106] Gerdoni, E., Gallo, B., Casazza, S., Musio, S. et al., Mesenchymal stem cells effectively modulate pathogenic immune response in experimental autoimmune encephalomyelitis. *Ann. Neurol.* 2007, *61*, 219–227.

[107] Gordon, D., Pavlovska, G., Glover, C. P., Uney, J. B. et al., Human mesenchymal stem cells abrogate experimental allergic encephalomyelitis after intraperitoneal injection, and with sparse CNS infiltration. *Neurosci. Lett.* 2008, *448*, 71–73.

[108] Kassis, I., Grigoriadis, N., Gowda-Kurkalli, B., Mizrachi-Kol, R. et al., Neuroprotection and immunomodulation with mesenchymal stem cells in chronic experimental autoimmune encephalomyelitis. *Arch. Neurol.* 2008, *65*, 753–761.

[109] Uccelli, A., Laroni, A., Freedman, M. S., Mesenchymal stem cells for the treatment of multiple sclerosis and other neurological diseases. *Lancet Neurol.* 2011, *10*, 649–656.

[110] Uccelli, A., Moretta, L., Pistoia, V., Mesenchymal stem cells in health and disease. *Nat. Rev. Immunol.* 2008, *8*, 726–736.

[111] Prockop, D. J., Repair of tissues by adult stem/progenitor cells (MSCs): controversies, myths, and changing paradigms. *Mol. Ther.* 2009, *17*, 939–946.

[112] Ortiz, L. A., Gambelli, F., McBride, C., Gaupp, D. et al., Mesenchymal stem cell engraftment in lung is enhanced in response to bleomycin exposure and ameliorates its fibrotic effects. *Proc. Natl. Acad. Sci. USA* 2003, *100*, 8407–8411.

[113] Ortiz, L. A., DuTreil, M., Fattman, C., Pandey, A. C. et al., Interleukin 1 receptor antagonist mediates the antiinflammatory and antifibrotic effect of mesenchymal stem cells during lung injury. *Proc. Natl. Acad. Sci. USA* 2007, *104*, 11002–11007.

[114] Kunter, U., Rong, S., Djuric, Z., Boor, P. et al., Transplanted mesenchymal stem cells accelerate glomerular healing in experimental glomerulonephritis. *J. Am. Soc. Nephrol.* 2006, *17*, 2202–2212.

[115] Lee, R. H., Seo, M. J., Reger, R. L., Spees, J. L. et al., Multipotent stromal cells from human marrow home to and promote repair of pancreatic islets and renal glomeruli in diabetic pancreatic islets and renal glomeruli in diabetic NOD/scid mice. *Proc. Natl. Acad. Sci. USA* 2006, *103*, 17438–17443.

[116] Minguell, J. J., Erices, A., Mesenchymal stem cells and the treatment of cardiac disease. *Exp. Biol. Med.* 2006, *231*, 39–49.

[117] Phinney, D. G., Isakova, I., Plasticity and therapeutic potential of mesenchymal stem cells in the nervous system. *Curr. Pharm. Des.* 2005, *11*, 1255–1265.

[118] Fischer, U. M., Harting, M. T, Jimenez, F., Monzon-Posadas, W. O. et al., Pulmonary passage is a major obstacle for intravenous stem cell delivery: the pulmonary first-pass effect. *Stem. Cells Dev.* 2009 *18*, 683–692.

[119] Bruno, S., Grange, C., Deregibus, M. C., Calogero, R. A. et al., Mesenchymal stem cell-derived microvesicles protect against acute tubular injury. *J. Am. Soc. Nephrol.* 2009, *20*, 1053–1067.

[120] Bruno, S., Grange, C., Collino, F., Deregibus, M. C. et al., Microvesicles derived from mesenchymal stem cells enhance survival in a lethal model of acute kidney injury. *PLoS One* 2012, *7*, e33115.

[121] Gatti, S., Bruno, S., Deregibus, M. C., Sordi, A. et al., Microvesicles derived from human adult mesenchymal stem cells protect against ischaemia-reperfusion-induced acute and chronic kidney injury. *Nephrol. Dial. Transplant.* 2011, *26*, 1474–1483

[122] He, J., Wang, Y., Sun, S., Yu, M. et al., Bone marrow stem cells-derived microvesicles protect against renal injury in the mouse remnant kidney model. *Nephrology* 2012, *17*, 493–500.

[123] Ranganath, S. H., Levy, O., Inamdar, M. S., Karp, J. M., Harnessing the mesenchymal stem cell secretome for the treatment of cardiovascular disease. *Cell Stem Cell.* 2012, *10*, 244–258.

[124] Lai, R. C., Chen, T. S., Lim, S. K., Mesenchymal stem cell exosome: a novel stem cell-based therapy for cardiovascular disease. *Regen. Med.* 2011, *6*, 481–492.

[125] Mummery, C. L., Davis, R. P., Krieger, J. E., Challenges in using stem cells for cardiac repair. *Sci. Transl. Med.* 2010, *2*, 27ps17.

[126] Wollert, K. C., Drexler, H., Cell therapy for the treatment of coronary heart disease: a critical appraisal. *Nat. Rev. Cardiol.* 2010, *7*, 204–215.

[127] Timmers, L., Lim, S. K., Arslan, F., Armstrong, J. S. et al., Reduction of myocardial infarct size by human mesenchymal stem cell conditioned medium. *Stem Cell Res.* 2007, *1*, 129–137.

[128] Lai, R. C., Arslan, F., Lee, M. M., Sze, N. S. et al., Exosome secreted by MSC reduces myocardial ischemia/reperfusion injury. *Stem Cell Res.* 2010, *4*, 214–222.

[129] Lai, R. C., Arslan, F., Tan, S. S., Tan, B. et al., Derivation and characterization of human fetal MSCs: an alternative cell source for large-scale production of cardioprotective microparticles. *J. Mol. Cell Cardiol.* 2010, *48*, 1215–1224.

[130] Xin, H., Li, Y., Buller, B., Katakowski, M. et al., Exosome-mediated transfer of miR-133b from multipotent mesenchymal stromal cells to neural cells contributes to neurite outgrowth. *Stem Cells* 2012, *30*, 1556–1564.

[131] Honmou, O., Onodera, R., Sasaki, M., Waxman, S. G., Kocsis, J. D., Mesenchymal stem cells: therapeutic outlook for stroke. *Trends Mol. Med.* 2012, *18*, 292–297.

[132] Dreyer, J. L., New insights into the roles of microRNAs in drug addiction and neuroplasticity. *Genome Med.* 2010, *2*, 92.

[133] Katsuda, T., Tsuchiya, R., Kosaka, N., Yoshioka, Y. et al., Human adipose tissue-derived mesenchymal stem cells secrete functional neprilysin-bound exosomes. *Sci. Rep.* 2013, *3*, 1197.

[134] Kim, H. S., Choi, D. Y., Yun, S. J., Choi, S. M. et al., Proteomic analysis of microvesicles derived from human mesenchymal stem cells. *J. Proteome Res.* 2012, *11*, 839–849.

[135] Veevers-Lowe, J., Ball, S. G., Shuttleworth, A., Kielty, C. M., Mesenchymal stem cell migration is regulated by fibronectin through α5β1-integrin-mediated activation of PDGFR-β and potentiation of growth factor signals. *J. Cell Sci.* 2011, *124*, 1288–1300.

[136] Chan, J., O'Donoghue, K., Gavina, M., Torrente, Y. et al., Galectin-1 induces skeletal muscle differentiation in human fetal mesenchymal stem cells and increases muscle regeneration. *Stem Cells* 2006, *24*, 1879–1891.

[137] Kishore, R., Qin, G. J., Luedemann, C., Bord, E. et al., The cytoskeletal protein ezrin regulates EC proliferation and angiogenesis via TNF-alpha-induced transcriptional repression of cyclin A. *J. Clin. Invest.* 2005, *115*, 1785–1796.

[138] Meyer, R. D., Sacks, D. B., Rahimi, N., IQGAP1-dependent signaling pathway regulates endothelialcellproliferation and angiogenesis. *PLoS One* 2008, *3*, e3848.

[139] Chen, T. S., Lai, R. C., Lee, M. M., Choo, A. B. et al., Mesenchymal stem cell secretes microparticles enriched in pre-microRNAs. *Nucleic Acids Res.* 2010, *38*, 215–224.

[140] Akerblom, M., Sachdeva, R., Jakobsson, J., Functional Studies of microRNAs in neural stem cells: problems and perspectives. *Front. Neurosci.* 2012, *6*, 14.

[141] Fang, M., Wang, J., Zhang, X., Geng, Y. et al., The miR-124 regulates the expression of BACE1/β-secretase correlated with cell death in Alzheimer's disease. *Toxicol. Lett.* 2012, *209*, 94–105.

[142] Collino, F., Deregibus, M.C., Bruno, S., Sterpone, L. et al., Microvesicles derived from adult human bone marrow and tissue specific mesenchymal stem cells shuttle selected pattern of miRNAs. *PloS One* 2010, *5*, e11803.

[143] Herrera, M.B., Bruno, S., Buttiglieri, S., Tetta, C. et al., Isolation and characterization of a stem cell population from adult human liver. *Stem Cells* 2006, *24*, 2840–2850.

[144] Herrera, M. B., Fonsato, V., Gatti, S., Deregibus, M. C. et al. Human liver stem cell-derived microvesicles accelerate hepatic regeneration in hepatectomized rats. *J. Cell. Mol. Med.* 2010, 1605–1618.

[145] Stärkel, P., De Saeger, C., Sempoux, C., Legrand, E. et al., Blunted DNA synthesis and delayed S-phase entry following inhibition of Cdk2 activity in the regenerating rat liver. *Lab. Invest.* 2005, *85*, 562–571

[146] Amzallag, N., Passer, B. J., Allanic, D., Segura, E. et al., TSAP6 facilitates the secretion of translationally controlled tumor protein/histamine-releasing factor via a nonclassical pathway. *J. Biol. Chem.* 2004, *279*, 46104–46112.

[147] Yu, X., Harris, S. L., Levine, A. J., The regulation of exosome secretion: a novel function of the p53 protein. *Cancer Res.* 2006, *66*, 4795–4801.

[148] Alonso, R., Rodríguez, M. C., Pindado, J., Merino, E. et al., Diacylglycerol kinase α regulates the secretion of lethal exosomes bearing Fas ligand during activation-induced cell death of T lymphocytes. *J. Biol. Chem.* 2005, *280*, 28439–28450.

[149] Islam, A., Shen, X., Hiroi, T., Moss, J. et al., The brefeldin A-inhibited guanine nucleotide-exchange protein, BIG2, regulates the constitutive release of TNFR1 exosome-like vesicles. *J. Biol. Chem.* 2007, *282*, 9591–9599.

[150] Parolini, I., Federici, C., Raggi, C., Lugini, L. et al., Microenvironmental pH is a key factor for exosome traffic in tumor cells. *J. Biol. Chem.* 2009, *284*, 34211–34222.

[151] Alvarez-Erviti, L., Seow, Y., Yin, H., Betts, C. et al., Delivery of siRNA to the mouse brain by systemic injection of targeted exosomes. *Nat. Biotechnol.* 2011, *29*, 341–345.

[152] Miyanishi, M., Tada, K., Koike, M., Uchiyama, Y. et al., Identification of Tim4 as a phosphatidylserine receptor. *Nature* 2007, *450*, 435–439.

[153] Feng, D., Zhao, W. L., Ye, Y. Y., Bai, X. C. et al., Cellular internalization of exosomes occurs through phagocytosis. *Traffic* 2010, *11*, 675–687.

[154] Fitzner, D., Schnaars, M., van Rossum, D., Krishnamoorthy, G. et al., Selective transfer of exosomes from oligodendrocytes to microglia by macropinocytosis. *J. Cell Sci.* 2011, *124*, 447–458.

[155] Ciravolo, V., Huber, V., Ghedini, G. C., Venturelli, E. et al., Potential role of HER2-overexpressing exosomes in countering Trastuzumab-based therapy. *J. Cell. Physiol.* 2012, *227*, 658–667.

[156] Malam, Y., Loizidou, M., Seifalian, A. M., Liposomes and nanoparticles: nanosized vehicles for drug delivery in cancer. *Trends Pharmacol. Sci.* 2009, *30*, 592–599.

[157] Zhuang, X., Xiang, X., Grizzle, W., Sun, D. et al., Treatment of brain inflammatory diseases by delivering exosome encapsulated anti-inflammatory drugs from the nasal region to the brain. *Mol. Ther.* 2011, *19*, 1769–1777.

 DOI: 10.1002/eji.201343531 Eur. J. Immunol. 2013. 43: 2956–2968

European Journal of Immunology

Adipose tissue derived stromal stem cell therapy in murine ConA-derived hepatitis is dependent on myeloid-lineage and CD4+ T-cell suppression

Mami Higashimoto[*1], *Yoshio Sakai*[*2,3], *Masayuki Takamura*[1], *Soichiro Usui*[1], *Alessandro Nasti*[1], *Keiko Yoshida*[1], *Akihiro Seki*[1], *Takuya Komura*[1], *Masao Honda*[3], *Takashi Wada*[2], *Kengo Furuichi*[4], *Takahiro Ochiya*[5] *and Shuichi Kaneko*[1,3]

[1] Disease Control and Homeostasis, Kanazawa University, Kanazawa, Japan
[2] Department of Laboratory Medicine, Kanazawa University, Kanazawa, Japan
[3] Department of Gastroenterology, Kanazawa University Hospital, Kanazawa, Japan
[4] Division of Blood Purification, Kanazawa University Hospital, Kanazawa, Japan
[5] Division of Molecular and Cellular Medicine, National Cancer Center Research Institute, Tokyo, Japan

Mesenchymal stromal stem cells (MSCs) are an attractive therapeutic model for regenerative medicine due to their pluripotency. MSCs are used as a treatment for several inflammatory diseases, including hepatitis. However, the detailed immunopathological impact of MSC treatment on liver disease, particularly for adipose tissue derived stromal stem cells (ADSCs), has not been described. Here, we investigated the immunomodulatory effect of ADSCs on hepatitis using an acute ConA C57BL/6 murine hepatitis model. i.v. administration of ADSCs simultaneously or 3 h post injection prevented and treated ConA-induced hepatitis. Immunohistochemical analysis revealed higher numbers of CD11b+, Gr-1+, and F4/80+ cells in the liver of ConA-induced hepatitis mice was ameliorated after the administration of ADSCs. Hepatic expression of genes affected by ADSC administration indicated tissue regeneration-related biological processes, affecting myeloid-lineage immune-mediating Gr-1+ and CD11b+ cells. Pathway analysis of the genes expressed in ADSC-treated hepatic inflammatory cells revealed the possible involvement of T cells and macrophages. TNF-α and IFN-γ expression was downregulated in hepatic CD4+ T cells isolated from hepatitis livers co-cultured with ADSCs. Thus, the immunosuppressive effect of ADSCs in a C57BL/6 murine ConA hepatitis model was dependent primarily on the suppression of myeloid-lineage cells and, in part, of CD4+ T cells.

Keywords: Adipose tissue derived stromal stem cells · Anti-inflammatory effects · CD4+ T cells · ConA hepatitis · Myeloid-lineage cells

Additional supporting information may be found in the online version of this article at the publisher's web-site

Correspondence: Dr. Shuichi Kaneko
e-mail: skaneko@m-kanazwa.jp

*These authors contributed equally to this work.

Introduction

Mesenchymal stromal stem cells (MSCs) are somatic cells that reside in the mesenchymal tissues, such as the BM, umbilical cord, and adipose tissue [1,2]. MSCs are able to differentiate into several types of cells (pluripotent) in the same lineage, such as chondrocytes, osteocytes, adipocytes, and cardiomyocytes, as well as those of different lineages, such as hepatocytes. Because of this differentiation capability, they have been studied as a possible application in regenerative therapy of miscellaneous impaired organs, such as breast reconstruction [3] and repair of ischemic heart tissue [4]. Another intriguing characteristic of MSCs is their immunomodulatory potency [5]. Because most liver diseases, including viral hepatitis [6,7], primary biliary cirrhosis [8], autoimmune hepatitis [9], and steatohepatitis [10], are associated with hepatic inflammatory cells [11], elucidation of the effect of MSCs on hepatic inflammation is important when considering the use of MSCs for treating liver diseases. Although the efficacy of MSC treatment of liver diseases has been reported [12], the detailed immunopathological impact of MSC treatment on liver diseases, particularly for adipose tissue derived stromal stem cells (ADSCs), has not been investigated.

ConA, a plant lectin [13], is frequently used to induce acute hepatitis in rodents [14] to model the pathological features of autoimmune hepatitis. Although this model is mediated mainly by lymphocyte-lineage cells such as T cells and NKT cells, Kupffer cells/macrophages also participate in hepatitis. Therefore, evaluating the therapeutic efficacy of ADSCs in this murine hepatitis model is important. Although the potential efficacy of ADSCs in a BALB/c ConA hepatitis model has been reported [15], the immunopathology has not been investigated.

We confirmed that immediate i.v. administration of ADSCs after ConA injection prevented hepatitis. We also observed that administering ADSCs 3 h after the ConA injection resulted in successful treatment of hepatitis, as the liver was already infiltrated by $CD11b^+$ and $Gr\text{-}1^+$ inflammatory cells. Gene expression analysis of the liver showed that ADSC treatment affected myeloid-lineage cells, providing repair and regenerative effects in ConA-induced hepatitis mice. Moreover, gene expression analysis of hepatic inflammatory cells indicated pathways related to T cells and monocyte-lineage cells. Pathologically important cytokines such as TNF-α and IFN-γ were upregulated in $CD4^+$ T cells isolated from ConA-induced hepatitis mice but were significantly suppressed by co-culture with ADSCs. Thus, the anti-inflammatory effects of ADSCs in the C57BL/6 murine ConA hepatitis model were mediated by the suppression of myeloid-lineage and $CD4^+$ T cells.

Results

Characteristics of the immune response in ConA-induced hepatitis mice

To examine the characteristics of ConA-induced acute hepatitis, we injected 300 μg ConA into C57BL/6 female mice ($n = 4$) and determined serum alanine transferase (ALT) and lactate dehydrogenase (LDH) activities. Serum ALT and LDH activities were elevated through 24 h (Fig. 1A). The macroscopic appearance and histology of the liver obtained 24 h after ConA injection revealed intense necrosis (Fig. 1B). The immunohistochemical analysis showed that the number of $CD4^+$ T cells in the liver peaked at 6 h after the ConA injection, and remained high for 24 h (Fig. 1C and D). The numbers of $CD11b^+$ cells and $Gr\text{-}1^+$ cells accumulated in the liver increased at 3 h and reached a maximum at 12 h after ConA injection (Fig. 1C and D). The numbers of $F4/80^+$ monocyte/macrophage lineage cells increased at 6 h after the ConA injection, but returned to basal levels after 24 h (Fig. 1C and D). We also assessed the frequency of $CD11b^+/Gr\text{-}1^+$ cells, as a phenotype of myeloid-derived suppressor cells (MDSCs), in ConA hepatitis mice at 6 h ($n = 3$). The frequency of $CD11b^+/Gr\text{-}1^+$ cells was higher than that in WT mice (Fig. 1E). Scavenger receptor CD204 expression was higher in $CD11b^+/Gr\text{-}1^+$ cells than $CD11b^+/Gr\text{-}1^-$ cells (Fig. 1F), and the population gated for $CD11b^+$ cells contained granulocytic $Ly\text{-}6C^+/Ly\text{-}6G^+$ cells as well as monocytic $Ly\text{-}6C^+/Ly\text{-}6G^-$ cells (Fig. 1G).

To determine the type of immune-mediating cells involved in ConA-induced acute hepatitis, we depleted mice of various immune cell subpopulations ($n = 4$ per group). Mice that were pretreated with clodronate, a reagent that depletes monocyte-macrophage lineage cells [16], followed by injection of ConA, did not show a significant elevation in serum ALT or LDH activity (Fig. 1H). Mild elevation of serum activity for these enzymes in mice depleted of $CD4^+$ T cells was observed, whereas depletion of $CD8^+$ T cells had no significant effect. These results suggest the importance of monocyte-macrophage myeloid-lineage cells, as well as the contribution of $CD4^+$ T cells, in ConA-induced hepatitis.

ConA-induced acute hepatitis is ameliorated by i.v. administration of ADSCs in vivo

Next, we determined the therapeutic efficacy of ADSCs in the ConA-induced hepatitis model. We obtained and expanded stromal cells from adipose tissue by passaging them eight to ten times (Fig. 2A). Almost all cells expressed the mesenchymal lineage markers, CD29 and CD44 (Fig. 2B). With regard to stem cell markers [17], approximately 40% and 73% of cells expressed CD105 and CD90, respectively (Fig. 2B). Moreover, the cells were pluripotent and were able to differentiate into osteocytes, chondrocytes, and adipocytes (Fig. 2C–F). When 1×10^5 ADSCs were administered via the tail vein immediately after ConA injection in mice ($n = 3$), the elevation of serum ALT and LDH activity was substantially ameliorated, compared with mice without ADSC treatment ($n = 4$) 24 h after injection (Fig. 3A). In terms of therapeutic efficacy, 1×10^5 ADSCs were administered to mice 3 h after ConA injection ($n = 3$), serum ALT and LDH activities were significantly reduced in acute hepatitis mice treated with ADSCs, compared with ConA-induced hepatitis mice without treatment ($n = 4$), 24 h after ConA administration (Fig. 3B). The macroscopic

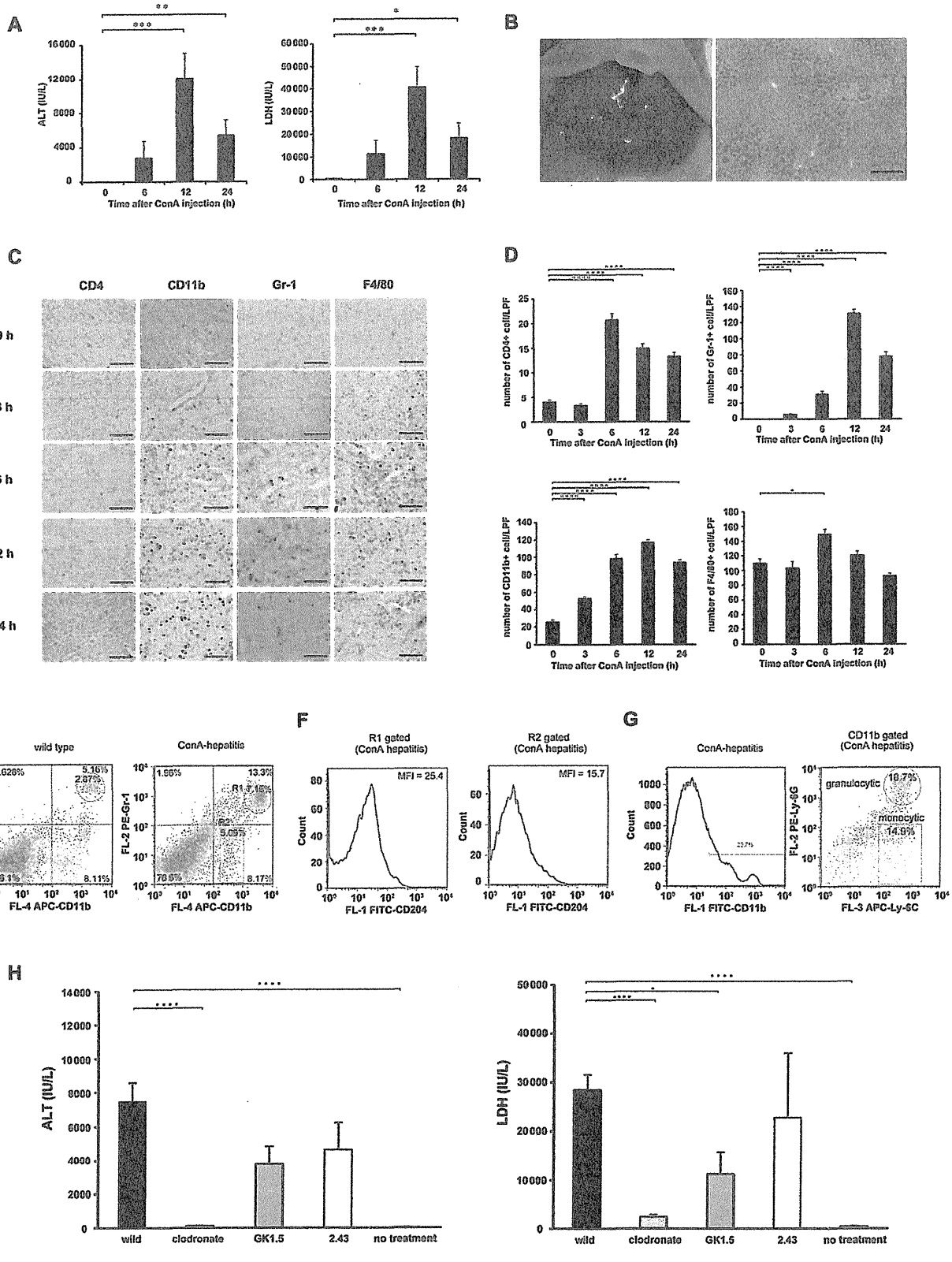

appearance of the liver obtained from mice injected with 300 μg of ConA followed by ADSC administration showed a mild and spotty white area with an almost normal color (Fig. 3C). Liver histology showed an almost normal appearance, with no necrosis (Fig. 3C), indicating that ConA-induced hepatitis was markedly ameliorated by ADSC treatment. No preventive or therapeutic effect on ConA-induced hepatitis resulted from administration of primary cultured murine hepatocytes ($n = 3$); there was no significant reduction in serum ALT or LDH (Fig. 3A and B), macroscopic necrosis appearance, or histological necrosis, compared with ConA-induced hepatitis (Fig. 3C).

ADSC treatment reduces elevated cytokine/chemokine concentrations in ConA-induced hepatitis mice

Marked protective and therapeutic effects of ADSCs on ConA-induced hepatitis were observed. To determine the effect of ADSC treatment on systemic inflammation in ConA-induced hepatitis, we measured serum cytokine and chemokine concentrations in ConA-induced hepatitis mice treated with ADSCs. Mice injected with ConA were immediately treated with ADSCs and serum was collected 6 h after ConA injection ($n = 3$). The elevated serum IFN-γ, IL-2, IL-6, IL-4, IP-10, MIG, KC, and MCP-1 levels in ConA-injected mice ($n = 3$) were significantly reduced by ADSC treatment (Supporting Information Fig. 1A). Injection of mice with ADSCs 3 h after ConA administration ($n = 4$) resulted in significantly reduced serum IFN-γ, IL-2, IL-6, and MIG levels, compared to ConA-injected mice not treated with ADSCs ($n = 6$) (Supporting Information Fig. 1B). Thus, the levels of the array of cytokines and chemokines that are elevated in the sera of ConA-induced hepatitis mice were significantly decreased by ADSC treatment.

Distribution of i.v. administered ADSCs in ConA-induced hepatitis murine models

The distribution of administered ADSCs in ConA-induced hepatitis mice was determined by immunohistochemistry. Administered GFP-expressing ADSCs were observed in the lung, but not the liver, of mice injected with ConA followed by immediate ADSC administration ($n = 6$), through 24 h (Supporting Information Fig. 2A). When administered to mice 3 h after ConA injection ($n = 6$), GFP-expressing ADSCs were observed primarily in the lung, and a few in the liver (Supporting Information Fig. 2B), suggesting that some fraction of ADSCs reached the liver upon occurrence of hepatitis.

Hepatic gene expression changes by ADSCs treatment are associated with Gr-1$^+$ and CD11b$^+$ cells

To investigate the detailed biological features of the liver in ConA-induced hepatitis mice that were treated with ADSCs, we examined the gene expression profiles of liver tissue of ConA-injected mice obtained 2 h after treatment with ADSCs using a DNA microarray. In the liver tissues of mice treated with ADSCs immediately after ConA injection ($n = 3$), 589 gene probes were differentially expressed compared with that in mice with ConA-induced hepatitis that had not been treated with ADSCs ($n = 3$). Expression of the majority of genes was downregulated by ADSCs, as shown by green color ($p < 0.05$; Fig. 4A). Principal component analysis using these genes showed a discernible distribution difference between the ADSC-treated and -untreated groups (Fig. 4B). When mice received ADSC treatment 3 h after ConA injection, hepatic expression of 309 gene probes was altered significantly compared with those in mice with ConA-induced hepatitis that had not been treated with ADSCs ($n = 3$). Expression of the majority of genes was downregulated by ADSCs, as shown by green color ($p < 0.01$; Fig. 4C). Principal component analysis of these genes also showed a discernible distribution difference between the ADSC-treated and untreated groups (Fig. 4D). In the context of biological maps of the genes affected by immediate ADSC treatment, cell differentiation, the inflammatory response, the DNA damage response, and apoptosis predominated (Supporting Information Table 1). In addition to these maps, tissue remodeling and wound repair, mitogenic signaling, and vascular development (angiogenesis) predominated in mice that had received ADSC treatment 3 h after ConA injection (Table 1), indicating that ADSCs provided not only anti-inflammatory effects, but also remodeling effects, in the ConA-damaged liver.

◀ **Figure 1.** Characteristics of ConA-induced hepatitis in C57BL/6 mice. (A–D) C57BL/6 female mice were injected i.v. with 300 μg of ConA. Sera and liver tissues were obtained 3, 6, 12, and 24 h after ConA injection. The data are representative of three individual experiments. (A) ALT and LDH activity in sera. Results are expressed as means ± SE ($n = 4$). $^*p < 0.05$, $^{**}p < 0.01$, $^{***}p < 0.005$ versus 0 h (Student's *t*-test). (B) Representative liver tissues obtained 12 h after ConA injection were assessed macroscopically and microscopically. Magnification: ×100. Bar: 200 μm. (C) Immunohistochemical staining for CD4, CD11b, Gr-1, and F4/80 in the livers of mice for each time point (0, 3, 6, 12, and 24 h; $n = 4$ per time point). Representative images of mice for each time point are shown. Magnification: ×100. Bar: 200 μm. (D) Quantification of the number of CD4$^+$, CD11b$^+$, Gr-1$^+$, and F4/80$^+$ cells in four visual fields per ×100 low-power field in the livers of representative mice in each group. Magnification: ×100. $^*p < 0.05$, $^{***}p < 0.001$ versus untreated mice (Student's *t*-test). (E–G) Hepatic inflammatory cells were isolated from mice 6 h after ConA injection, incubated with fluorescence-conjugated antibodies, and assessed by FACS. Three mice per group per experiment. Experiments were performed twice. (E) Frequency of CD11b$^+$Gr-1$^+$ cells in WT C57BL/6 mice and ConA hepatitis mice. (F) Analysis of CD204 expression in CD11b$^+$Gr-1$^+$ cells (R1-gated region in (E)) and CD11b$^+$Gr-1$^-$ cells (R2-gated region in (E)) among hepatic inflammatory cells from ConA hepatitis mice. MFI: mean fluorescence intensity. (G) CD11b$^+$ cells among hepatic inflammatory cells from ConA hepatitis mouse were gated, and Ly-6C and Ly-6G expression levels in the gated cells were determined. (H) C57BL/6 female mice were injected i.v. with clodronate ($n = 4$), i.p. with anti-CD4 antibody (GK1.5) ($n = 4$), or anti-CD8 antibody (2.43) ($n = 4$) every 24 h for 2 days. The mice were then injected i.v. with 300 μg of ConA. Sera were obtained 24 h after ConA injection, and ALT and LDH activities were then measured. Results are expressed as means +SE ($n = 4$ per group) and are representative of one experiment performed. $^*p < 0.05$, $^{****}p < 0.001$ versus ConA-injected WT mice ($n = 4$) (Student's *t*-test).

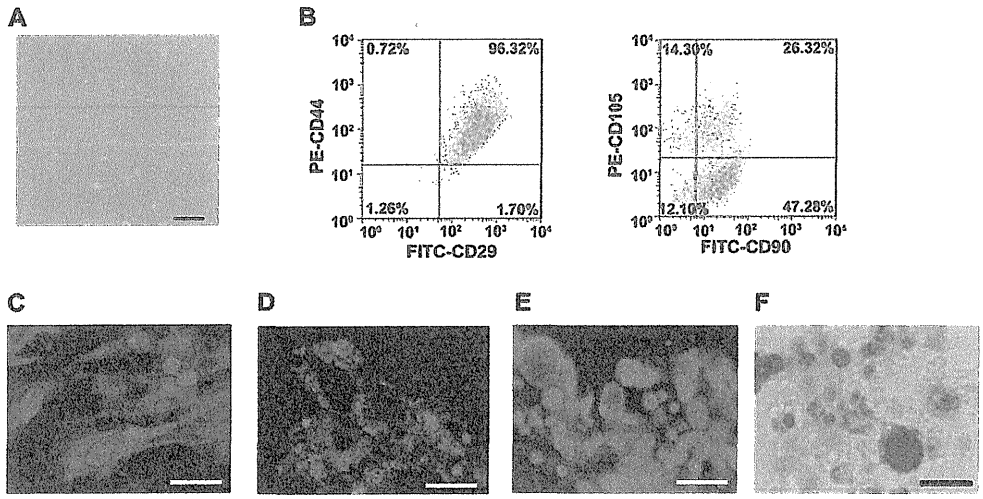

Figure 2. Characteristics and pluripotency of cultured ADSCs. Cells in the stromal fraction of adipose tissues from mice were cultured, maintained, and expanded for eight to ten passages. (A) Spindle shaped cells were observed after eight passages. Magnification: ×100. Bar: 200 μm. (B) Flow cytometric analysis of CD29, CD44, CD90, and CD105 surface marker expression. The data shown are representative of three independent experiments. (C–F) ADSCs were cultured with specific growth factors for induction of osteocytes, chondrocytes, and adipocytes using a mouse mesenchymal stem cell functional kit. Immunohistochemical staining was performed with (C) anti-osteopontin antibody for osteocytes, (D) anti-collagen II antibody for chondrocytes, and (E) anti-FABP antibody as well as (F) Oil-Red O staining for adipocytes. Magnification: x200. Bars: 50 μm. All data shown are from one experiment representative of two independent experiments performed.

Next, we investigated the relevance of these altered genes in the context of inflammatory cells using the public gene expression database of hematopoietic cells and stem cells (GSE27787). The annotated genes among the 589 gene probes detected by microarray analysis probes in the livers of mice that received ADSC treatment immediately after ConA injection were not relevant to any hematopoietic cell type (Fig. 4E). By contrast, among the 309 gene probes, the majority of the annotated genes whose hepatic expression in mice that received ADSC treatment 3 h after ConA injection was affected significantly were found to be highly expressed in Gr-1$^+$ cells and Mac1$^+$ (CD11b$^+$) cells — as indicated by the red color (Fig. 4F). Since majority of the 309 gene probes in the liver of ConA hepatitis were downregulated by ADSC treatment, as indicated by green color (Fig. 4C), these results suggested that effects on Gr-1$^+$ and CD11b$^+$ cells were associated with the therapeutic effect of ADSCs 3 h after ConA injection.

ADSC treatment represses inflammatory cell accumulation in ConA-induced hepatitis

To determine the influence of ADSC treatment on the infiltration/accumulation of immune-mediating cells in the liver of ConA-induced hepatitis mice, we assessed by immunohistochemistry the inflammatory cells in the liver tissues of mice injected with ConA followed by ADSC administration at 3 h. Liver tissues obtained at 6, 12, and 24 h ($n = 4$ each time point) after ConA injection showed reduced accumulation of CD11b$^+$ cells, Gr-1$^+$ cells, and F4/80$^+$ cells after ADSC treatment (Fig. 5). In contrast, the increased number of infiltrated CD4$^+$ T cells in ConA-induced hepatitis mice was not significantly affected by the ADSCs (Fig. 5). Thus, the predominant change in ConA-induced hepatitis mice treated with ADSCs was in the number of myeloid-lineage inflammatory cells, consistent with the hepatic gene expression data.

T-cell involvement in the altered gene expression of hepatic inflammatory cells by ADSCs treatment

To further assess the anti-inflammatory effects of ADSCs in mice with ConA-induced hepatitis, we isolated hepatic inflammatory cells from mice 2 h after ADSC treatment, which was administered 3 h after ConA injection ($n = 2$) and from mice not treated with ADSCs ($n = 2$). A total of 939 genes were differentially expressed in hepatic inflammatory cells from ConA-induced hepatitis mice treated with ADSCs. The gene expression profiles associated with ADSC treatment and ConA-induced hepatitis without ADSC treatment were readily distinguishable (Supporting Information Fig. 3A). Pathway map analysis showed that these genes were relevant to biological pathways of oncostatin M signaling via JAK-Stat or MAPK signaling and CCR5 signaling in macrophages and T lymphocytes in the immune response pathway (Supporting Information Table 2). Network analysis of these genes featured a network consisting of AcRIIA, STAT3, Activin A, FTSJD1, and STAT1 at the top (Supporting Information Table 3), which indicated that pathways involving IL-2 and TNF-α, and the STAT1/STAT3 pathway were also involved (Supporting Information Fig. 3B). These results suggest that T cells, as well as antigen presenting/phagocytosis lineages, were the immune-mediating cell populations affected by ADSC treatment.

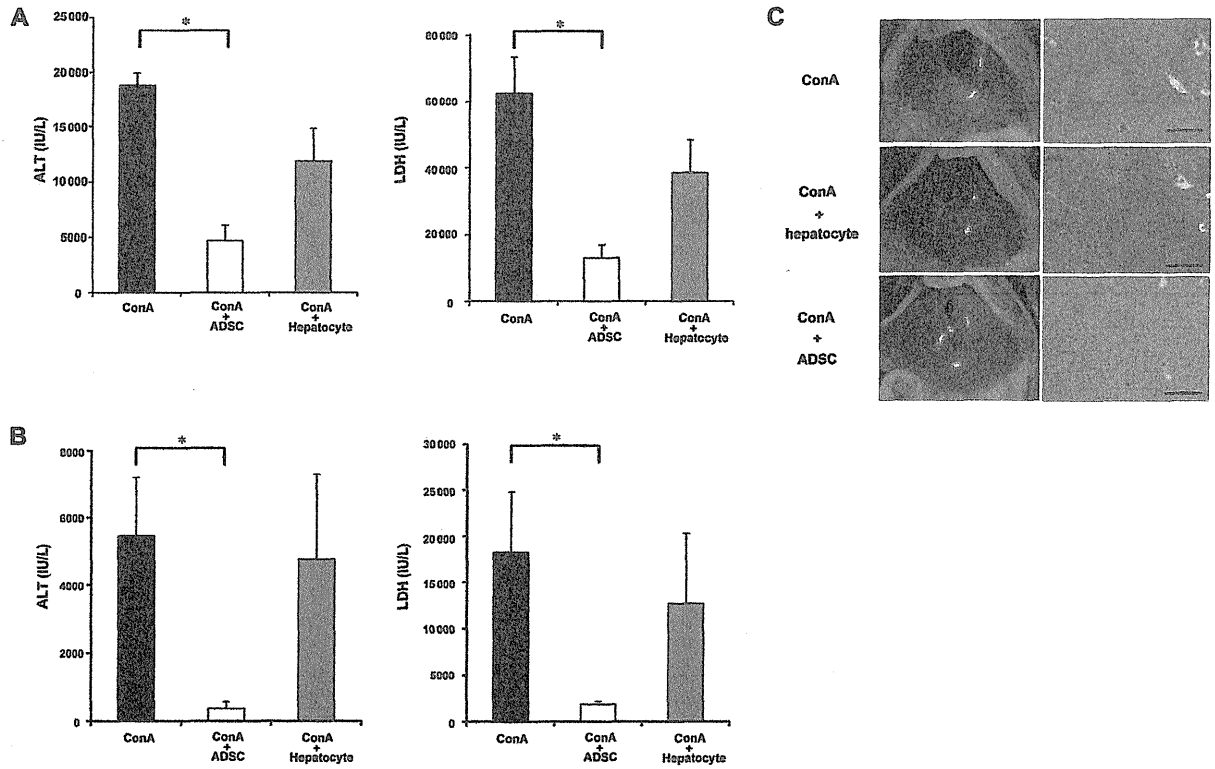

Figure 3. Therapeutic effects of ADSCs in ConA-induced hepatitis. C57BL/6 female mice were injected i.v. with 300 μg of ConA. Immediately or 3 h later, 1×10^5 ADSCs or hepatocytes were injected via the tail vein. Liver tissues and blood samples were obtained 24 h after ConA injection. Liver tissues were examined histologically and serum ALT and LDH activities were measured. (A, B) Serum ALT and LDH activities of mice injected with ConA followed by ADSC injection (A) immediately or (B) 3 h later. ConA: ConA-injected mice without treatment ($n = 4$), ConA + ADSC: ConA-injected mice followed by ADSC treatment ($n = 3$), ConA + hepatocyte: ConA-injected mice followed by primary cultured hepatocyte treatment ($n = 3$). Data are shown as mean ± SE and are from one experiment representative of two independent experiments. $^*p < 0.05$ (Wilcoxon signed-rank test), compared with ConA-injected mice. (C) Macroscopic appearance of the liver (left) and histology of the liver tissues as assessed by H&E staining (right). Magnification of histology: ×100. Bars: 200 μm. Images shown are from one mouse representative of three to four mice from each group studied.

ConA-activated CD4$^+$T cells and CD11b$^+$ cells in the liver are important targets of ADSC treatment

The above data indicated that ADSCs administered in ConA-induced hepatitis had therapeutic immunological effects in terms of repairing the damaged liver and affected CD11b$^+$ and Gr-1$^+$ myeloid-lineage cells and T cells. To further explore how ADSCs affected the subpopulations of inflammatory cells involved in ConA-induced hepatitis, we investigated the expression of cytokine/chemokine-related genes in CD4$^+$ T cells and CD11b$^+$ cells obtained from livers with ConA-induced hepatitis ($n = 4$) that had been treated in vitro with ADSCs ($n = 3$). Expression of TNF-α, IL-10, and CXCL10 was significantly downregulated by ADSC treatment in both CD4$^+$ T cells (Supporting Information Fig. 4A) and CD11b$^+$ cells (Supporting Information Fig. 4B). IFN-γ, IL-4, and CXCL9 expression by CD4$^+$ T cells were significantly affected by ADSCs. Although CCL3, which was upregulated by ConA injection, was not significantly affected by ADSCs, the expression of its cognate receptor, CCR5, was decreased in CD4$^+$ T cells (Supporting Information Fig. 4A), suggesting an effect on the CCL3-CCR5 axis. These results suggest that CD4$^+$ T cells and myeloid-lineage CD11b$^+$ cells were the susceptible hepatic inflammatory subpopulations of cells in the ConA-induced hepatitis liver.

Anti-inflammatory effect of ADSCs on ConA hepatitis do not rely on MDSCs

We further assessed whether the anti-inflammatory effect of ADSCs in ConA hepatitis relied on MDSCs. Neither the frequency of nor the NO production by CD11b$^+$Gr-1$^+$ cells were increased by ADSC treatment (Supporting Information Fig. 5A). CD11b$^+$Gr-1$^+$ cells from ConA-injected mice treated with ADSCs showed arginase activity similar to that in CD11b$^+$Gr-1$^+$ cells from ConA-injected mice (Supporting Information Fig. 5B). CD11b$^+$Gr-1$^+$ cells from ConA-injected mice treated with ADSCs suppressed the ConA-stimulated proliferation of T cells in vitro, although the effect was slightly attenuated compared to that of cells from mice with ConA-induced hepatitis (Supporting Information Fig. 5C). Thus, ADSC treatment was not dependent on MDSCs induced by ConA hepatitis.

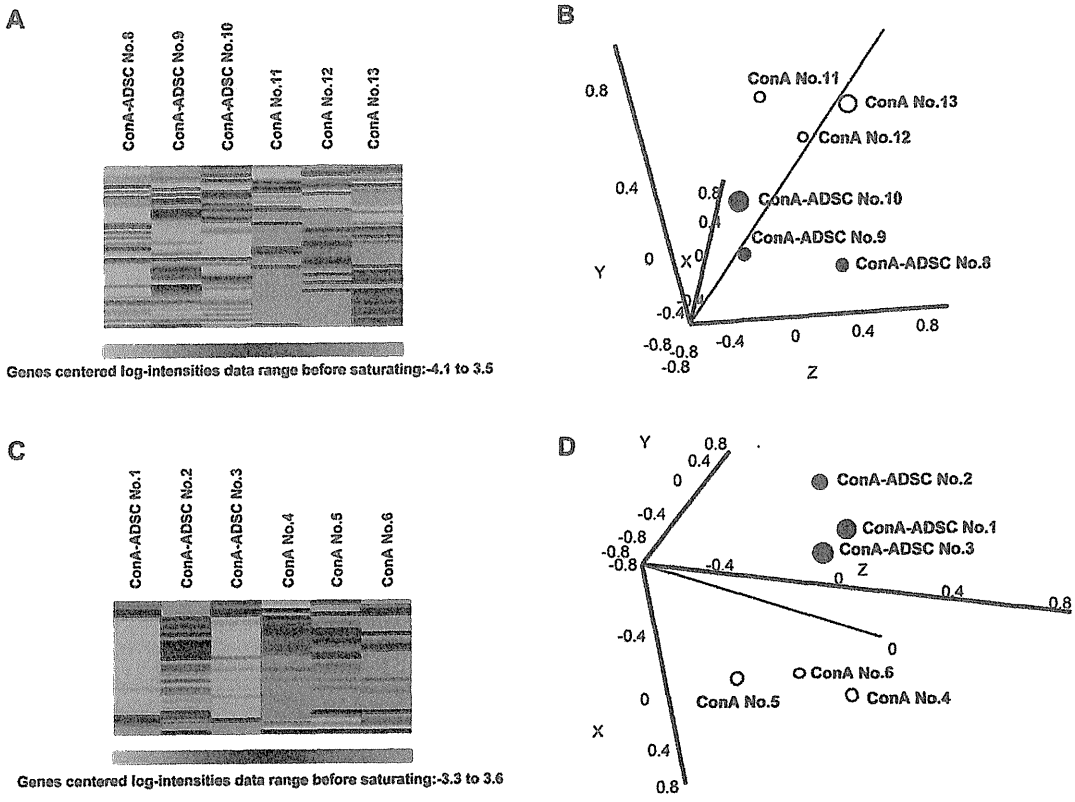

Discussion

MSCs are effective for immune-mediated disease treatment including the ConA-induced BALB/c murine hepatitis model [15], but the detailed mechanisms have not been fully elucidated. Here, we confirmed that ADSCs have preventive and therapeutic effects in a ConA-induced C57BL/6 hepatitis murine model and assessed the immunopathological mechanisms by determining the participating hepatic immunomodulatory cells. ADSCs injected via the tail vein were found in the lung; some were observed in the liver but only when ADSCs were administered 3 h after ConA injection, a time at which infiltration of $CD11b^+$ and $Gr\text{-}1^+$ inflammatory cells into the liver had already begun. Gene expression analysis of liver tissue from ConA-induced hepatitis mice showed that the ADSC treatment induced biological pathways indicative of liver repair and regeneration. Myeloid-lineage cells were the predominant population in terms of affected genes, consistent with immunohistochemical staining of the liver for immune-mediating cells. Furthermore, the gene expression profiles of hepatic inflammatory cells from ConA-induced hepatitis mice treated with ADSCs suggested T-cell and macrophage involvement. Moreover, the expression patterns of cytokine/chemokine-related genes in hepatic inflammatory cells co-cultured with ADSCs suggested that $CD4^+$ T cells were important in ConA-induced hepatitis and were affected by ADSC treatment.

The immunopathological features of ConA-induced hepatitis have been characterized as being primarily lymphocyte-lineage cell-mediated hepatitis [18–20], leading to massive hepatocellular degeneration, necrosis, and apoptosis [21]; thus, this model is relevant to clinical autoimmune hepatitis. Additionally, Kupffer cells play an important role in induction of hepatitis [22]. Unexpectedly, we observed prominent increases in $CD11b^+$, $Gr\text{-}1^+$, and $F4/80^+$ cells in liver tissues of the ConA-induced hepatitis mice. Additionally, we found that the monocyte-macrophage lineage cells contributed most significantly to hepatitis, as confirmed by depletion treatment, such that hepatitis was almost completely abolished when those cell types were abrogated by clodronate. This is further evidenced by the fact that ADSC treatment reduced the number of $CD11b^+$, $Gr\text{-}1^+$, and $F4/80^+$ cells in the liver of ConA-induced hepatitis mice (Fig. 5). The importance of $Gr\text{-}1^+$ and $CD11b^+$ cells was also suggested by changes in the gene expression profile of the liver of ConA-induced hepatitis treated with ADSCs (Fig. 4C and F). Thus, monocyte-macrophage lineage cells are important in the pathogenesis of ConA-induced hepatitis in mice and are important targets of ADSCs. $CD4^+$ T cells were also involved since their depletion partially ameliorated ConA-induced hepatitis. The number of infiltrating $CD4^+$ T cells in the liver of ConA-induced hepatitis mice was not markedly reduced by ADSC treatment. However, gene expression analysis of hepatic inflammatory cells in ConA-induced hepatitis mice treated with ADSCs showed that signaling of oncostatin M, a type I cytokine associated with developing T cells [23], and CCR5 signaling in macrophages and T lymphocytes were affected. Therefore, $CD4^+$ T cells participate as an immune mediator and therapeutic target of ADSCs in the pathology of ConA-induced hepatitis mice.

With regard to cytokine/chemokine-related gene expression in hepatic inflammatory cells of ConA-induced hepatitis mice, expression of TNF-α, IL-10, and CXCL10 in $CD4^+$ T cells and $CD11b^+$ cells was downregulated by ADSC treatment (Supporting Information Fig. 4). Additionally, IFN-γ, IL-4, and CXCL9 were also significantly downregulated in $CD4^+$ T cells, but not in $CD11b^+$ cells (Supporting Information Fig. 4). Changes in the expression of the Th2 cytokines, IL-10 and IL-4, were considered to be the secondary consequence of ConA-induced hepatitis, mediated by TNF-α and/or IFN-γ, which are characterized as Th1-associated cytokines [24]. CCR5 expression by $CD4^+$ T cells was downregulated by ADSCs, which may be relevant to the biological processes indicated by the downregulated genes in hepatic inflammatory cells. Because CCR5 is a $CD4^+$ T-cell receptor that interacts with APCs, such as macrophages [25], suppression of CCR5 expression on $CD4^+$ T cells by ADSC might explain the amelioration of ConA-mediated hepatitis. Overall, the therapeutic efficacy of ADSCs impacted both $CD4^+$ and $CD11b^+$ cells in terms of alteration of levels of inflammatory humoral mediators and cytokine/chemokine profiles, thus contributing to amelioration of ConA-induced hepatitis.

A proportion of i.v. administered ADSCs were present in the livers of ConA mice injected with ADSCs at a time point at which the liver had already been infiltrated with $Gr\text{-}1^+$ and $CD11b^+$ cells, whereas no ADSCs were present in the livers of mice injected with ConA following immediate treatment with ADSCs. This indicates that a liver undergoing inflammation attracts administered ADSCs. The extent of inflammation required to recruit ADSCs should be clarified, as it has previously been reported that hepatitis occurring just 30 min after ConA injection results in recruitment of a substantial number of stem cells to the liver in the BALB/c ConA hepatitis model [15]. Given that the migratory capabilities of MSCs are well known although not yet fully investigated [26], how ADSCs are recruited to an already inflamed liver as a result of ConA administration should be examined. In addition, the ADSCs administered to C57BL/6 mice immediately after ConA injection resided in the lung. In spite of the fact that they were not detected in the liver, these ADSCs prevented ConA hepatitis, indicating the remote effect of ADSCs. Thus, indirect mediators produced by ADSCs associated with their anti-inflammatory effects should be investigated intensively.

Figure 4. Gene expression analysis in the liver of ConA-induced hepatitis mice treated with ADSCs. C57BL/6 female mice were injected i.v. with 300 μg of ConA. (A, B, and E) Immediately or (C, D, and F) 3 h after ConA injection, mice were treated with 1×10^5 ADSCs via the tail vein ($n = 3$ each). Liver tissues were analyzed 2 h after ADSC administration and RNA was isolated for gene expression analysis using a DNA microarray. Data shown are from one experiment performed. (A, B) One-way clustering analysis (A) and principal component analysis (B) of the 589 differentially expressed genes in treated and untreated ConA-injected mice. (C, D) One-way clustering analysis (C) and principal component analysis (D) of the 309 differentially expressed genes in treated (after 3 h) and untreated ConA-injected mice followed. Colors indicate the intensity of gene upregulation (red), downregulation (green), and no change (black). (E, F) One-way clustering analysis of gene expression in hematopoietic and stem cells (GSE27787) for annotated genes among the 589 (E) and 309 (F) genes.

Table 1. Maps relevant to genes for which the expression was affected in the liver of ConA-injected mice followed by ADSC treatment at 3 h.

Maps	*p*-value
Tissue remodeling and wound repair	0.000001438
Inflammatory response	0.000003973
Mitogenic signaling	0.0001056
Vascular development (angiogenesis)	0.0002926
DNA damage response	0.0004529
Apoptosis	0.0008909
Cystic fibrosis disease	0.001402
Myogenesis regulation	0.001571
Cell differentiation	0.002173
Immune system response	0.003304

In conclusion, the therapeutic anti-inflammatory efficacy of ADSCs relied on suppression of myeloid-lineage and $CD4^+$ T cells in the ConA-induced C57BL/6 murine hepatitis model. The application of ADSC therapy to various inflammatory liver diseases can be further developed by studies of their immunomodulatory effects.

Materials and methods

Murine acute hepatitis induced by ConA injection and treatment with ADSCs

C57BL/6J female mice (10–12 weeks old, Charles River Laboratories Japan Inc., Yokohama, Japan) were injected i.v. with 300 μg of ConA (Sigma-Aldrich, St. Louis, MO, USA) dissolved in PBS. For $CD4^+$ T-cell or $CD8^+$ T-cell depletion, 200 μg of purified anti-CD4 antibody from the culture supernatant of GK1.5 cells (ATCC, Manassas, VA, USA), or purified anti-CD8 antibody from the culture supernatant of 2.43 cells (ATCC), was injected i.p. for two consecutive days before ConA injection. For depletion of monocyte-macrophage lineage cells, 2 mg of clodronate (Sigma-Aldrich), which was encapsulated in liposomes using the COATSOME-EL-01-N liposome formulation kit (Nihonyushi, Tokyo, Japan) [27], was injected via the tail vein 2 days before ConA injection. For the prevention or treatment experiment, 1×10^5 ADSCs were administered i.v. immediately or 3 h after ConA injection. In some cohorts, blood was obtained under anesthesia, and liver and lung tissues were collected after euthanizing mice at 6, 12, and 24 h after ConA injection. A portion of the liver tissue was homogenized and the enriched fraction of inflammatory cells was obtained by gradient centrifugation using Ficoll–Hypaque (Sigma-Aldrich). Our institutional review board approved the care and use of laboratory animals in all experiments.

Isolation and culture of ADSCs and primary hepatocytes

Inguinal adipose tissues were obtained from C57BL/6J male mice (10–12 weeks old, Charles River Laboratories Japan Inc.) or GFP-transgenic mice (male, 10–12 weeks old, gift from Prof. Okabe, Osaka University, Japan). Tissues were digested with 0.075% collagenase type I (Wako Pure Chemical Industries Ltd., Osaka, Japan), washed with PBS, and then transferred to a culture dish with DMEM/F-12 1:1 medium (Life Technologies–Invitrogen, Carlsbad, CA, USA) supplemented with 10% heat-inactivated FBS and 1% antibiotic–antimycotic solution (Life Technologies). Cells were maintained and expanded by eight to ten passages before use.

To obtain primary hepatocytes, C57BL/6J male mice (10–12 weeks old) were anesthetized by i.p. injection of pentobarbital (50 mg/kg; Kyoritsu Seiyaku, Tokyo, Japan) and injected with 10 mL of 0.75% type I collagenase solution via the portal vein. Liver tissues were minced to dissociate cells, filtered through a 100 μm mesh, and cultured in 10-cm culture dishes for 16 h until use.

Pluripotency of ADSCs

The pluripotency of ADSCs was examined using a mouse mesenchymal stem cell functional kit® (R&D Systems, Minneapolis, MN, USA), and immunohistochemical staining of cells that had differentiated into osteocytes, chondrocytes, and adipocytes was performed using anti-mouse ostepontin, anti-mouse collagen II, and anti-mouse FABP4 antibodies, respectively, in accordance with the manufacturer's instruction. Adipocyte differentiation was also assessed by staining using an aliquot of Oil Red O (WAKO).

Co-culture of ConA-stimulated hepatic inflammatory cells with ADSCs

Hepatic inflammatory cells were isolated from C57BL/6J female mice (10 weeks old) that had been injected i.v. with 300 μg of ConA 3 h before ($n = 4$). $CD4^+$ T cells and $CD11b^+$ cells were separated from the collected hepatic inflammatory cells using anti-CD4 and anti-CD11b magnetic beads (Miltenyi Biotec, Bergisch Gladbach, Germany). Then, 20 000 ADSCs were co-cultured with 4×10^5 of the isolated $CD4^+$ T cells or $CD11b^+$ cells in a 24-well plate (BD Falcon, San Jose, CA, USA) for 2 h ($n = 3$). After co-culture, floating cells were harvested, and RNA harvested using the MicroRNA isolation kit (Stratagene, La Jolla, CA, USA) for real-time PCR analysis to measure cytokine/chemokine gene expression.

Measurement of serum ALT and LDH activity

Blood was collected from the postorbital venous plexus and serum was separated from clotted blood after coagulation. The serum activity of ALT, and LDH was measured using L-type WAKO GPT J2, and LDH-J kits (Wako Pure Chemical Industries Ltd.), respectively, using autoanalytical equipment (Hitach7180, Hitachi Ltd., Tokyo, Japan), according to the manufacturer's protocol.

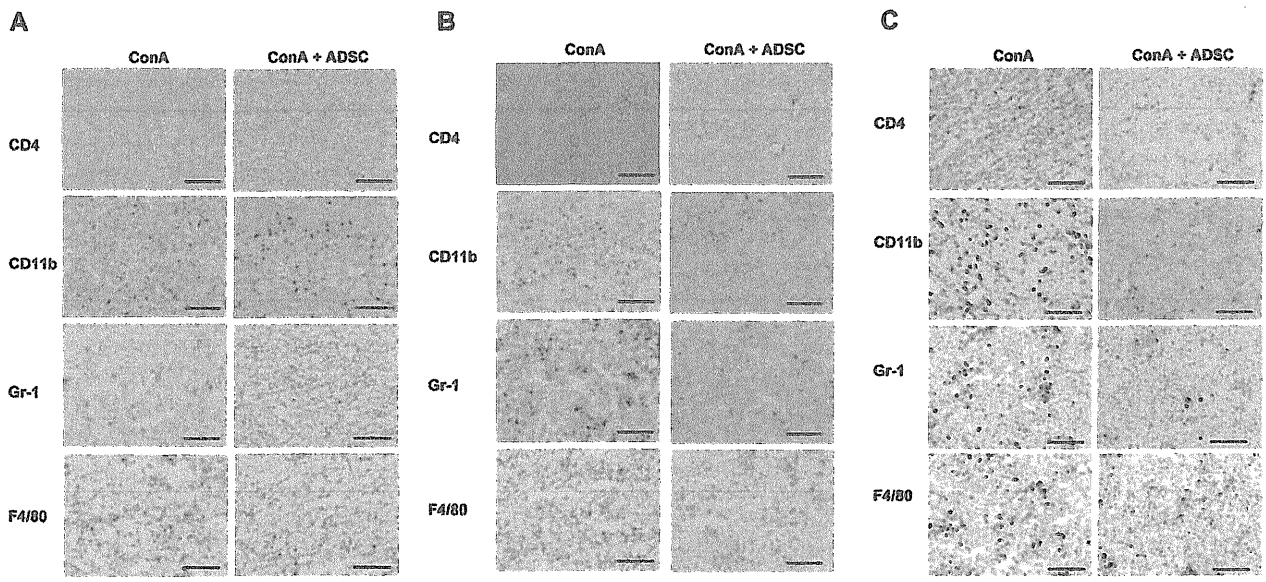

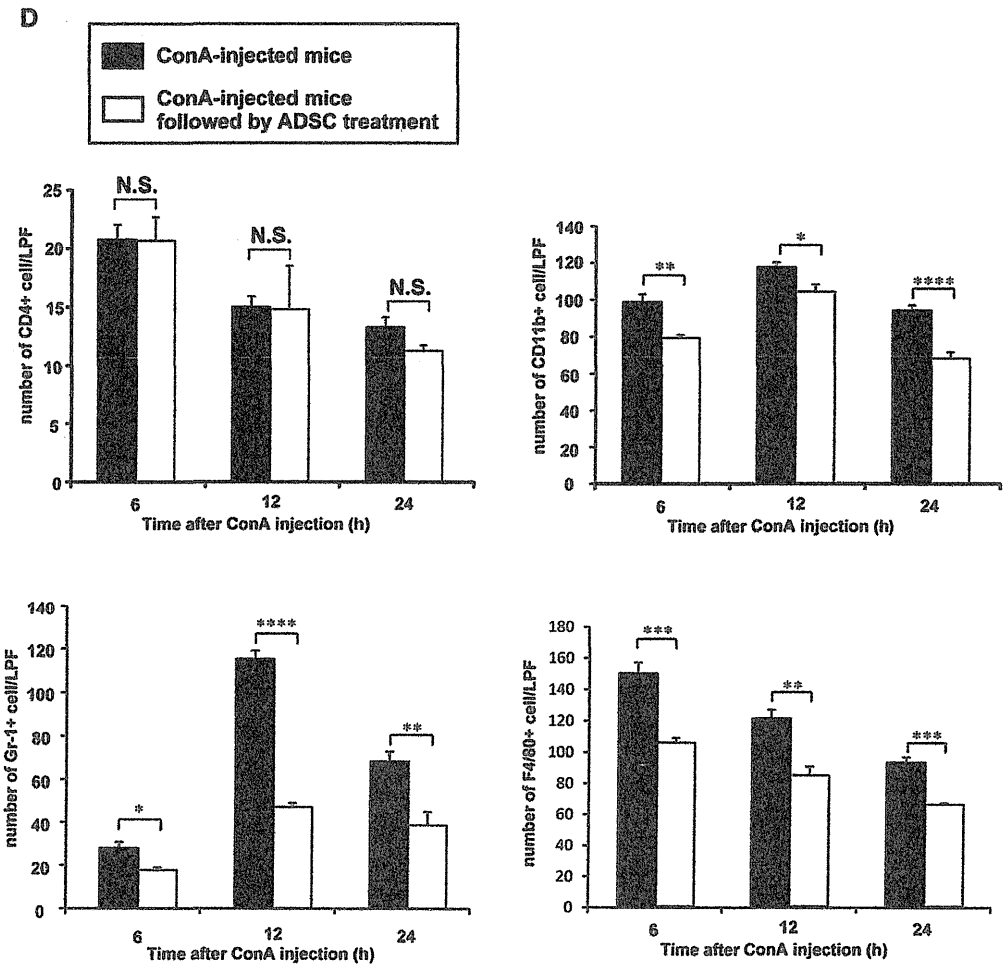

Measurement of serum cytokine/chemokine concentrations

Sera were obtained from ADSC-treated mice immediately or 3 h after ConA injection ($n = 3$ and $n = 4$, respectively), and from ConA-injected mice not treated with ADSCs ($n = 3$ and $n = 6$, respectively) at 6 h. Serum concentrations of cytokines and chemokines were measured using a Multiplex Bead Immunoassays kit, Mouse Cytokine 20-Plex Panel (Invitrogen, Carlsbad, CA, USA), following the manufacturer's protocol. The kit covers FGF-basic, GM-CSF, IFN-γ, IL-1α, IL-1β, IL-2, IL-4, IL-5, IL-6, IL-10, IL-12 (p40/p70), IL-13, IL-17, IP-10(CXCL10), KC, MCP-1, MIG(CXCL9), MIP-1α, TNF-α, and VEGF.

Histological and immunohistochemical analyses of liver and lung tissues

Harvested liver and lung tissues were fixed in 10% formaldehyde, embedded in paraffin, sectioned at 4 μm, and stained with H&E. For immunohistochemical analysis, the liver tissues were embedded in OCT compound (Sakura Finetek, Torrance, CA, USA), snap-frozen in liquid nitrogen, cryostat-sectioned, and fixed with methanol/acetone (1:1). The paraffin-embedded tissues were also sliced into 4 μm sections, mounted on microscope slides, and deparaffinized, followed by epitope retrieval using proteinase K (Dako, Glostrup, Denmark). The slides were incubated with peroxidase blocking reagent (Dako) for 15 min at room temperature to inhibit endogenous peroxidase activity, followed by incubation with protein blocking reagent (Dako) to avoid nonspecific protein reactions. The slides were incubated with primary antibodies (anti-mouse CD4, CD11b, Gr-1, F4/80) (BD Pharmingen, San Diego, CA, USA) and anti-GFP (MBL, Nagoya, Japan) diluted with PBS containing 1% BSA overnight at 4°C. After washing in PBS, the slides were then incubated with secondary antibodies (anti-rat, anti-rabbit; Nichirei, Japan) for 30 min at room temperature. The immune complexes were visualized using EnVision kits /HRP (DAB; Dako) followed by counterstaining with hematoxylin. The numbers of positive cells in each section were counted in four randomly selected fields at 100× magnification under a microscope.

RNA isolation and gene expression analysis by DNA microarray

Total RNA was obtained from the tissues or hepatic inflammatory cells in RNAlater (Ambion) using RNA isolation kit (Sigma-Aldrich) in accordance with the supplied protocol with slight modifications. Isolated RNA was amplified and labeled with the Cy3 using the Quick Amp labeling kit (Agilent Technologies, Santa Clara, CA, USA) in accordance with the manufacturer's protocol. cRNA of 1.65 μg was hybridized onto a Whole Mouse Genome 4 × 44K Array (Agilent Technologies) and scanned using a DNA Microarray Scanner (model G2505B, Agilent Technologies).

Gene expression data were analyzed using the GeneSpring analysis software (Agilent Technologies). Each measurement was divided by the 75th percentile of all measurements in that sample at per chip normalization. Hierarchical clustering and principal component analysis of gene expression was performed. Welch's *t*-test, with Benjamini and Hochberg's false discovery rate, was used to identify genes that were differentially expressed in the groups of interest. Analysis of biological processes was performed using the MetaCore software suite (GeneGo, Carlsbad, CA, USA). BRB array tools (http://linus.nci.nih.gov/BRB-ArrayTools.html) were also used for unsupervised or one-way clustering analyses. Microarray data were deposited in the NBCI Gene Expression Omnibus (GSE ID: GSE41465).

Flow cytometry

Cultured ADSCs were incubated in PBS supplemented with 2% BSA (Sigma-Aldrich) containing antibodies labeled with FITC or PE anti-mouse CD44 or CD90 (Beckman Coulter, Brea, CA, USA), and CD105 (Miltenyi Biotec) antibodies. Hepatic inflammatory cells isolated from mice were incubated with a mixture of FITC-labeled anti-mouse CD204 (AbD Serotec, Raleigh, NC, USA), PE-labeled anti-mouse Gr-1 (Miltenyi Biotec), and allophycocyanin-labeled anti-mouse CD11b (BioLegend, San Diego, CA, USA), or FITC-labeled anti-mouse CD11b (Beckman Coulter), PE-labeled anti-mouse Ly-6G (BioLegend), and allophycocyanin labeled anti-mouse Ly-6C (BioLegend) antibodies. The fluorescence intensity of the cells was measured using a FACSCalibur™ (Becton Dickinson, San Jose, CA, USA). Data obtained were visualized and analyzed using the FlowJo software (Tomy Digital Biology Co., Ltd., Tokyo, Japan).

Isolation of CD11b$^+$Gr-1$^+$ hepatic inflammatory cells and T-cell [3H]-thymidine incorporation assay

C57BL/6J female mice were injected with 300 μg of ConA and then injected with 1×10^5 ADSCs after 3 h ($n = 3$). Three

Figure 5. Immunohistochemical analysis of inflammatory cells in the liver of ConA-induced hepatitis mice treated with ADSCs. (A–C) Immunohistochemical staining of the liver. C57BL/6 female mice were injected i.v. with 300 μg of ConA. Then, 3 h later, the mice were injected with ADSCs via the tail vein. Liver tissues were obtained at (A) 6, (B)12, or (C) 24 h after ConA injection ($n = 4$ per each time point). Immunohistochemical staining was conducted using anti-CD4, anti-CD11b, anti-Gr-1, and anti-F4/80 antibodies. Stained liver images shown are representative of three experiments performed. Magnification: ×100. Bars: 200 μm. (D) Quantification of CD4$^+$, CD11b$^+$, Gr-1$^+$, and F4/80$^+$ cells in four visual fields per ×100 low-power field in the liver of representative mice from each group. Data are shown as mean +SE ($n = 4$) and are representative of three experiments performed. $^*p < 0.05$, $^{**}p < 0.01$, $^{***}p < 0.005$, $^{****}p < 0.001$; Student's *t*-test. n.s.: not significant.

hours later, hepatic inflammatory cells were isolated and incubated with FITC-labeled anti-mouse CD11b (Beckman Coulter) and PE-labeled anti-mouse Gr-1 (Miltenyi Biotec) antibodies. The $CD11b^+Gr\text{-}1^+$ population was collected using a FACSAira II™ (Becton Dickinson). $CD11b^+Gr\text{-}1^+$ cells (1×10^5), which had been irradiated with 2000 rads, were co-cultured with 1×10^5 purified splenic T cells isolated from C57BL/6J mice in RPMI1640 medium (Invitrogen) supplemented with 10% heat-inactivated FBS, 1% antibiotic–antimycotic solution (Life Technologies), and ConA (4 μg/mL) for 48 h ($n = 4$). The culture was pulsed with [3H]thymidine (1 μCi/well) for 16 h and harvested. Thymidine incorporation was measured using a beta-counter (PerkinElmer, Waltham, MA, USA).

NO assay

C57BL/6J female mice were injected with 300 μg of ConA. Three hours later, 1×10^5 ADSCs were injected via the tail vein. After a further 3 h, hepatic inflammatory cells were isolated from ConA hepatitis mice with or without ADSC treatment ($n = 3$ each) and incubated in PBS supplemented with 2% BSA, PE-labeled anti-mouse Gr-1 antibody, and allophycocyanin-labeled anti-mouse CD11b antibody. Cells were then incubated in PBS containing 2.5 mg/mL diaminofluorescein-FM diacetate (Sekisui Medical Co., Ltd., Tokyo, Japan), which emits fluorescence at 515 nm in a reaction with NO, at 37°C for 30 min and subjected to FACS analysis using a FACSCalibur flow cytometer.

Arginase assay

Female C57BL/6J mice were injected with 300 μg of ConA. Three hours later, 1×10^5 ADSCs were injected via the tail vein. After further 3 h, hepatic inflammatory cells were isolated from ConA hepatitis mice with or without ADSC treatment ($n = 3$ each) and were lysed with PBS containing 10 mM Tris-HCl (pH 7.4) and 0.4% Triton X-100, supplemented with the proteinase inhibitor cocktail, cOmplete, Mini, EDTA-free® (Roche, Basel, Switzerland). One hundred micrograms of the lysis aliquot obtained were subject to an arginase activity assay using a QuantiChrom™ Arginase Assay kit (BioAssay Systems, Hayward, CA), which measures urea produced from the substrate, in accordance with the manufacturer's protocol.

Statistical analysis

All data are expressed as means ± SE. Statistical analyses were performed using the JMP software (ver.9.02; SAS Institute Japan Inc., Tokyo, Japan). Student's *t*-test and Wilcoxon signed-rank test were used. p values < 0.05 were considered to indicate statistical significance.

Acknowledgements: This study was supported, in part, by subsidies from the Japanese Ministry of Education, Culture, Sports, Science, and Technology and the Japanese Ministry of Health, Labor, and Welfare.

Conflict of interest: The authors declare no financial or commercial conflict of interest.

References

1 Zuk, P. A., Zhu, M., Ashjian, P., De Ugarte, D. A., Huang, J. I., Mizuno, H., Alfonso, Z. C. et al., Human adipose tissue is a source of multipotent stem cells. *Mol. Biol. Cell* 2002. 13: 4279–4295.

2 Chamberlain, G., Fox, J., Ashton, B. and Middleton, J., Concise review: mesenchymal stem cells: their phenotype, differentiation capacity, immunological features, and potential for homing. *Stem Cells* 2007. 25: 2739–2749.

3 Perez-Cano, R., Vranckx, J. J., Lasso, J. M., Calabrese, C., Merck, B., Milstein, A. M., Sassoon, E. et al., Prospective trial of adipose-derived regenerative cell (ADRC)-enriched fat grafting for partial mastectomy defects: the RESTORE-2 trial. *Eur. J. Surg. Oncol.* 2012. 38: 382–389.

4 Janssens, S., Stem cells in the treatment of heart disease. *Annu. Rev. Med.* 2010. 61: 287–300.

5 Hoogduijn, M. J., Popp, F., Verbeek, R., Masoodi, M., Nicolaou, A., Baan, C. and Dahlke, M. H., The immunomodulatory properties of mesenchymal stem cells and their use for immunotherapy. *Int. Immunopharmacol.* 2010. 10: 1496–1500.

6 Baroni, G. S., Pastorelli, A., Manzin, A., Benedetti, A., Marucci, L., Solforosi, L., Di Sario, A. et al., Hepatic stellate cell activation and liver fibrosis are associated with necroinflammatory injury and Th1-like response in chronic hepatitis C. *Liver* 1999. 19: 212–219.

7 Cerny, A. and Chisari, F. V., Pathogenesis of chronic hepatitis C: immunological features of hepatic injury and viral persistence. *Hepatology* 1999. 30: 595–601.

8 Gershwin, M. E., Ansari, A. A., Mackay, I. R., Nakanuma, Y., Nishio, A., Rowley, M. J. and Coppel, R. L., Primary biliary cirrhosis: an orchestrated immune response against epithelial cells. *Immunol. Rev.* 2000. 174: 210–225.

9 Krawitt, E. L., Autoimmune hepatitis. *N. Engl. J. Med.* 1996. 334: 897–903.

10 Fujii, H. and Kawada, N., Inflammation and fibrogenesis in steatohepatitis. *J. Gastroenterol.* 2012. 47: 215–225.

11 Dienes, H. P. and Drebber, U., Pathology of immune-mediated liver injury. *Dig. Dis.* 2010. 28: 57–62.

12 Dai, L. J., Li, H. Y., Guan, L. X., Ritchie, G. and Zhou, J. X., The therapeutic potential of bone marrow-derived mesenchymal stem cells on hepatic cirrhosis. *Stem Cell Res.* 2009. 2: 16–25.

13 Sanders, D. A., Moothoo, D. N., Raftery, J., Howard, A. J., Helliwell, J. R. and Naismith, J. H., The 1.2 A resolution structure of the Con A-dimannose complex. *J. Mol. Biol.* 2001. 310: 875–884.

14 Kato, M., Ikeda, N., Matsushita, E., Kaneko, S. and Kobayashi, K., Involvement of IL-10, an anti-inflammatory cytokine in murine liver injury induced by concanavalin A. *Hepatol. Res.* 2001. 20: 232–243.

15 Kubo, N., Narumi, S., Kijima, H., Mizukami, H., Yagihashi, S., Hakamada, K. and Nakane, A., Efficacy of adipose tissue-derived mesenchymal stem cells for fulminant hepatitis in mice induced by concanavalin A. *J. Gastroenterol. Hepatol.* 2012. 27: 165–172.

16 Murdoch, C., Muthana, M., Coffelt, S. B. and Lewis, C. E., The role of myeloid cells in the promotion of tumour angiogenesis. *Nat. Rev. Cancer* 2008. 8: 618–631.

17 Banas, A., Teratani, T., Yamamoto, Y., Tokuhara, M., Takeshita, F., Quinn, G., Okochi, H. et al., Adipose tissue-derived mesenchymal stem cells as a source of human hepatocytes. *Hepatology* 2007. 46: 219–228.

18 Kaneko, Y., Harada, M., Kawano, T., Yamashita, M., Shibata, Y., Gejyo, F., Nakayama, T. et al., Augmentation of Valpha14 NKT cell-mediated cytotoxicity by interleukin 4 in an autocrine mechanism resulting in the development of concanavalin A-induced hepatitis. *J. Exp. Med.* 2000. 191: 105–114.

19 Tiegs, G., Hentschel, J. and Wendel, A., A T cell-dependent experimental liver injury in mice inducible by concanavalin A. *J. Clin. Invest.* 1992. 90: 196–203.

20 Halder, R. C., Aguilera, C., Maricic, I. and Kumar, V., Type II NKT cell-mediated anergy induction in type I NKT cells prevents inflammatory liver disease. *J. Clin. Invest.* 2007. 117: 2302–2312.

21 Schwabe, R. F. and Brenner, D. A., Mechanisms of liver injury. I. TNF-alpha-induced liver injury: role of IKK, JNK, and ROS pathways. *Am. J. Physiol. Gastrointest. Liver Physiol.* 2006. 290: G583–G589.

22 Schumann, J., Wolf, D., Pahl, A., Brune, K., Papadopoulos, T., van Rooijen, N. and Tiegs, G., Importance of Kupffer cells for T-cell-dependent liver injury in mice. *Am. J. Pathol.* 2000. 157: 1671–1683.

23 Clegg, C. H., Rulffes, J. T., Wallace, P. M. and Haugen, H. S., Regulation of an extrathymic T-cell development pathway by oncostatin M. *Nature* 1996. 384: 261–263.

24 Constant, S. L. and Bottomly, K., Induction of Th1 and Th2 CD4+ T cell responses: the alternative approaches. *Annu. Rev. Immunol.* 1997. 15: 297–322.

25 Contento, R. L., Molon, B., Boularan, C., Pozzan, T., Manes, S., Marullo, S. and Viola, A., CXCR4-CCR5: a couple modulating T cell functions. *Proc. Natl. Acad. Sci. USA* 2008. 105: 10101–10106.

26 Ponte, A. L., Marais, E., Gallay, N., Langonne, A., Delorme, B., Herault, O., Charbord, P. et al., The in vitro migration capacity of human bone marrow mesenchymal stem cells: comparison of chemokine and growth factor chemotactic activities. *Stem Cells* 2007. 25: 1737–1745.

27 Kushiyama, T., Oda, T., Yamada, M., Higashi, K., Yamamoto, K., Oshima, N., Sakurai, Y. et al., Effects of liposome-encapsulated clodronate on chlorhexidine gluconate-induced peritoneal fibrosis in rats. *Nephrol. Dial. Transplant.* 2011. 26: 3143–3154.

Abbreviations: **ADSC**: adipose tissue derived stromal stem cell · **ALT**: alanine transferase · **LDH**: lactate dehydrogenase · **MDSC**: myeloid-derived suppressor cell · **MSC**: mesenchymal stromal stem cell

Full correspondence: Dr. Shuichi Kaneko, Disease Control and Homeostasis, Kanazawa University, 13-1 Takara-machi, Kanazawa, Ishikawa 920-8641, Japan
Fax: +81-76-234-4250
e-mail: skaneko@m-kanazwa.jp

Received: 17/3/2013
Revised: 3/7/2013
Accepted: 6/8/2013
Accepted article online: 12/8/2013